Space Sci Rev (2010) 152: 341–390
DOI 10.1007/s11214-009-9580-z

Paleomagnetic Records of Meteorites and Early Planetesimal Differentiation

Benjamin P. Weiss · Jérôme Gattacceca · Sabine Stanley · Pierre Rochette · Ulrich R. Christensen

Received: 28 August 2009 / Accepted: 12 October 2009 / Published online: 15 December 2009

Abstract The large-scale compositional structures of planets are primarily established during early global differentiation. Advances in analytical geochemistry, the increasing diversity of extraterrestrial samples, and new paleomagnetic data are driving major changes in our understanding of the nature and timing of these early melting processes. In particular, paleomagnetic studies of chondritic and small-body achondritic meteorites have revealed a diversity of magnetic field records. New, more sensitive and highly automated paleomagnetic instrumentation and an improved understanding of meteorite magnetic properties and the effects of shock, weathering, and other secondary processes are permitting primary and secondary magnetization components to be distinguished with increasing confidence. New constraints on the post-accretional histories of meteorite parent bodies now suggest that, contrary to early expectations, few if any meteorites have been definitively shown to retain records of early solar and protoplanetary nebula magnetic fields. However, recent studies of pristine samples coupled with new theoretical insights into the possibility of dynamo generation on small bodies indicate that some meteorites retain records of internally generated fields. These results indicate that some planetesimals formed metallic cores and early dynamos within just a few million years of solar system formation.

Keywords Paleomagnetism · Planetary magnetic fields · Meteorites · Dynamo models · Differentiation

B.P. Weiss (✉)
Department of Earth, Atmospheric, and Planetary Sciences, Massachusetts Institute of Technology, 54-814, 77 Massachusetts Avenue, Cambridge, MA 02139, USA
e-mail: bpweiss@mit.edu

J. Gattacceca · P. Rochette
Centre Européen de Recherche et d'Enseignement des Géosciences de l'Environnement, Aix-Marseille Université-Centre National de la Recherche, PB80, 13545, Aix en Provence cedex 4, France

S. Stanley
Department of Physics, University of Toronto, 60 St. George Street, Toronto, ON M5S 1A7, Canada

U.R. Christensen
Max-Planck-Institut für Sonnensystemforschung, 37191 Katlenburg-Lindau, Germany

1 Introduction

Perhaps the most significant events in planetary history are those responsible for global planetary differentiation. These are the processes of large-scale melting and sequestration of compositionally distinct materials that give rise to a long-lived radially layered structure. Although planetary differentiation is occurring in a localized form even today on volcanically active bodies like Earth, Mars, and Io, the large-scale melting necessary for the formation of metallic cores overlain by silicate mantles and crusts occurred predominantly in the early solar system.

It is now well known that for large (greater than ∼2000 km radius) bodies, the gravitational energy of formation exceeds that required to completely melt the bodies, likely leading to the formation of surface magma oceans (Wetherill 1990; Pritchard and Stevenson 2000). Smaller bodies that formed early enough to accrete significant quantities of short-lived nuclides like ^{26}Al should have also experienced radiogenic heating sufficient for large-scale melting (Urey 1955; Hevey and Sanders 2006; Sahijpal et al. 2007). However, these bodies probably melted from the inside-out. Bodies that experienced greater than several tens of weight % melting have the potential to form metallic cores. The formation of cores is evident in the great diversity of iron meteorite groups and in the depletion of siderophile elements in a variety of basaltic achondrites groups (Haack and McCoy 2007; Mittlefehldt 2007). Hf/W chronometry indicates that these cores formed within 0–3 million years (Ma) after the formation of calcium aluminum inclusions (CAIs) (Kleine et al. 2005). These cores would have been initially molten, and if they cooled quickly, they may have convected (Chabot and Haack 2006). Convecting cores may have generated dynamo magnetic fields that could have magnetized the overlying silicate rocks (Weiss et al. 2008a). This magnetization, possibly recorded in meteorite samples today, can be studied by paleomagnetic techniques as a way to infer the history of planetesimal differentiation and field generation.

Paleomagnetic studies could also potentially provide a unique window into understanding early solar magnetic fields generated externally from planetesimal bodies. The T Tauri Sun and protoplanetary nebula are both thought to have been significant field generating sources during the first several Ma of solar system history (Collinson 1994; Balbus 2009). The large-scale steady dynamo field of T Tauri stars is thought to be approximately dipolar with typical surface fields of ∼0.1 T that fall off with the inverse cube of distance from the stellar center (Vallée 2003). Early magnetic fields associated with the early Sun and nebula may have slowed the Sun's rotation and permitted continued growth by accretion of disk material. The inner ionized region of the protoplanetary disk is thought to have been unstable to the magnetorotational instability (Balbus 2003, 2009), which likely generated spatially complex fields of up to ∼100 μT (Sano et al. 2004; Johansen 2009). The latter process may have been a critical source of turbulent viscosity that in turn is likely required for mass and momentum transfer in the disk and, ultimately, the formation of the Sun and planets. Stellar and MRI-generated fields, as well as residual fields from the parent molecular cloud and transient fields from possible nebular lightning- and impact-generated plasmas, may have also been intimately involved in the formation and/or magnetization of the earliest solar system macroscopic solids, inclusions and chondrules in chondrites (Levy and Araki 1989; Shu et al. 1996, 1997; Crawford and Schultz 1999; Desch and Cuzzi 2000; Desch and Connolly 2002; Joung et al. 2004). Despite their great importance in planet formation, there has been as yet no unambiguous evidence of any of these field sources in meteorites. However, new advances in rock magnetism and magnetic instrumentation suggest that future paleomagnetic studies offer the potential for identifying records of these fields in meteorites and their constituents.

Here we review recent advances in paleomagnetic studies of meteorites thought to be from small planetary bodies and recent theoretical work in small-body differentiation and dynamo generation. Our goal is to provide a detailed overview of the paleomagnetic record that has been studied over the last sixty years beginning with the first investigations of Anyzeski (1949), Levinson-Lessing (1952) and Fonton (1954) and the first detailed analyses of Lovering (1959) and Stacey and Lovering (1959). We examine both the growing modern database as well as revisit older data from a modern paleomagnetic and geomagnetic perspective. We focus on the natural remanent magnetization (NRM) of meteorites and only discuss rock magnetic properties as they relate to the interpretation of NRM. We do not discuss paleomagnetic studies of iron meteorites and pallasites due to their poorly understood magnetic field recording properties (e.g., Guskova 1965b; Brecher and Albright 1977; Nagata et al. 1987). We also do not discuss the extensive work in lunar (reviewed by Fuller 1974, 2007; Hood and Cisowski 1983; Fuller and Cisowski 1987; Dunlop and Ozdemir 1997; Wieczorek et al. 2006) and Martian paleomagnetism (see Rochette et al. 2001, 2005, 2006; Fuller 2007; Acuña et al. 2008) except as they relate to the general context of extraterrestrial paleomagnetism. Although most work on meteorites took place in the 1970s and early 1980s (see previous reviews by Levy and Sonett 1978; Hood and Cisowski 1983; Cisowski 1987; Collinson 1992, 1994; Dunlop and Ozdemir 1997; Fuller 2007; Rochette et al. 2009b), there has recently been a burst of activity brought on by advances in paleomagnetic techniques and instrumentation, an increasingly numerous and diverse sample suite, advances in dynamo theory, and perhaps most importantly, a growing petrologic and geochemical dataset that is providing crucial contextual and geochronological information for understanding the nature and origin of remanent magnetization.

We begin by discussing the technical difficulties specific to paleomagnetic studies of meteorites in Sect. 2. We assume the reader has a working knowledge of paleomagnetism and geomagnetism at the level of Butler (1992). We then review paleomagnetic studies of chondrites and achondrites in Sects. 3 and 4. In Sect. 5, we discuss the theoretical implications of meteorite paleomagnetism for small-body dynamos. We end in Sects. 6 and 7 by discussing outstanding questions and summarizing key conclusions.

2 Challenges in Interpreting the Meteorite Record

2.1 Geologic Context and Paleo-Orientation

The foremost challenge for meteorite paleomagnetic studies is that, unlike in earth science, the parent body, geologic context, and original orientation of nearly all samples are unknown. Other than lunar and Martian meteorites, the only two exceptions are the howardite-eucrite-diogenite (HED) clan, thought be from the asteroid 4 Vesta, and the anomalous ureilite Almahata Sitta, which was recently observed as an F-class asteroid prior to its landing on Earth (see Sect. 4). Even for these samples, the sampling site and orientation are unknown and the parent body is at the moment only barely resolved in telescope images (Thomas et al. 1992). As a result, extraterrestrial paleomagnetic studies have focused on measuring only the magnitude (and not the orientation) of the magnetization vector in order to recover the paleointensity of the field that magnetized the meteorites. This situation is very different from the field of terrestrial paleomagnetism, which has used paleo-orientation measurements to obtain a wealth of information about the Earth's field geometry, field temporal variability (e.g., geomagnetic reversals), and tectonic motions.

2.2 Scarcity of Material and Implications for Demagnetization Methods

Many meteorites are rare and little material is readily available for study. As a result, it is often difficult to obtain the large numbers of mutually oriented samples which are necessary for demonstrating primary magnetization. Those samples that are obtained are typically small in size and can therefore have relatively weak moments and substantial magnetic anisotropy. Another consequence is that often only nondestructive alternating field (AF) methods are permitted for demagnetization and paleointensity studies. AF methods are superior to thermal demagnetization in that they are ideally suited for removing common isothermal remanent magnetization (IRM) overprints from magnets (see Sect. 2.7). They also offer the advantage of not altering the meteorite's mineralogy, which permits the very same subsamples to be further analyzed with rock magnetic techniques and geochronometry. However, unlike thermal methods, AF methods do not unblock thermoremanent NRM in the same way that it was acquired, such that secondary thermal and viscous overprints sometimes cannot be easily isolated and highly accurate (∼10%) paleointensities cannot be measured.

AF methods (particularly those using static field treatments) also can introduce spurious anhysteretic remanent magnetization (ARM) and gyroremanent magnetization (GRM), both of which can mask the underlying NRM and falsely appear to be primary remanence (Collinson 1983; Stephenson 1993; Hu et al. 1998). Spurious acquisition of ARM, in which a directionally apparently random component is increasingly acquired during AF demagnetization due to imperfections in the AF-waveform (Fig. 1), has in fact been known for several decades (see Collinson 1983). This problem is particularly severe for studies of metal-bearing meteorites because the low coercivity of multidomain iron means that the NRM can be quickly masked by ARM-related noise. ARM noise can be reduced by making multiple AF steps at the same or similar peak fields and averaging the resulting directions (e.g., Cisowski 1991; Acton et al. 2007). New advances in measurement automation (Kirschvink et al. 2008) have recently enabled dozens of repeat measurements to be averaged, thereby permitting AF demagnetization of extraterrestrial samples to be carried up to unprecedented levels (Weiss et al. 2008a; Garrick-Bethell et al. 2009).

In contrast to ARM noise, GRM (Hu et al. 1998; Stephenson 1993) is only a recently discovered phenomenon. It is insidious in that it is typically acquired during AF demagnetization as a unidirectional component that could potentially be mistaken as a primary NRM. For example, a study of the angrite NWA 4931 (Weiss et al., unpublished data) found that the majority of subsamples had origin-trending NRM directions after AF demagnetization to ∼15 mT. However, some subsamples were susceptible to acquiring weak spurious ARM at AF steps above ∼10 mT and, more importantly, strong GRM above ∼30 mT (Fig. 1). This was manifested as a dramatic shallowing of the NRM directions and increase in moment during static three-axis AF treatment: GRM is acquired perpendicularly to the final (in this case, vertical) AF axis. Fortunately, GRM-correction methods (Dankers and Zijderveld 1981; Stephenson 1993; Hu et al. 1998), like measuring the moment after each uniaxial AF treatment, mitigate these effects and retrieve origin-trending magnetization (Fig. 1). Furthermore, GRM, because it grows with AF field, can generally be distinguished from primary NRM because it does not produce a characteristic magnetization decaying linearly to the origin. Given that GRM was only discovered in the early 1980s, well after most meteorite and lunar paleomagnetic studies, meteorite paleomagnetic data acquired before this time must be viewed with some caution. In fact, GRM has only been seriously considered in extraterrestrial paleomagnetic studies during just the last two years (Weiss et al. 2008a; Lawrence et al. 2008; Garrick-Bethell et al. 2009).

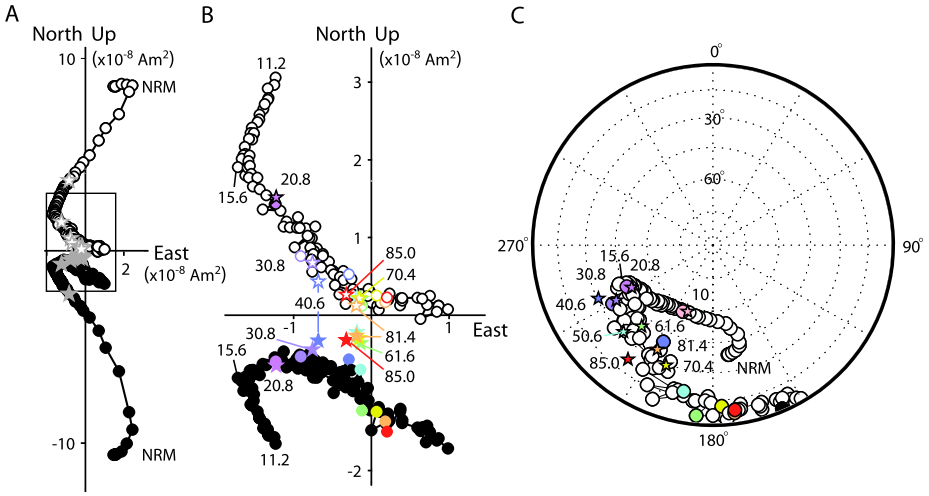

Fig. 1 Spurious ARM and GRM acquisition by angrite NWA 4931 during AF demagnetization. **A** Orthogonal demagnetization plot showing evolution of NRM vector during demagnetization. *Open and closed symbols* represent projections of the endpoint of the magnetization vector on vertical and horizontal planes, respectively. *Circles* = static three-axis (for NRM–AF 85 mT) or single z-axis (for AF 90 to 257.9 mT) demagnetization conducted in the axis order x (north–south), y (east–west), and z (up–down), with moment measurement taken after final (z) step only. *Stars* = NRM directions corrected for GRM using the Zijderveld–Dunlop method (Stephenson 1993) in which moment measurements taken after each of the three uniaxial AF demagnetization steps are averaged. GRM-corrected steps were only acquired every ~10–15 mT. *Boxed area* is magnified in **B**. **B** Close-up of *boxed area* in **A**. Selected demagnetization steps are listed in mT. After each GRM-corrected step, a static three-axis AF step with the same peak field was acquired. For a given AF field, the GRM-corrected and static three-axis AF steps share the same color (*lavender* = 20.8 mT, *purple* = 30.8 mT, *blue* = 40.6 mT, *light blue* = 50.6 mT, *green* = 61.6 mT, *yellow* = 70.4 mT, *red* = 85 mT). **C** Equal area projection showing directions of natural remanent magnetization corresponding to data in **A** and **B**. Color and symbols are the same as in **B**. The directional jitter around the mean NRM direction above ~15 mT is likely a manifestation of weak spurious ARM noise, while the dramatic increase in NRM and directional shallowing above 30 mT for static three-axis AF data are a manifestation of GRM. Weiss et al. (unpublished data)

2.3 Shock

Most meteorites have been shocked to peak pressures in excess of 5–10 GPa. For instance, Martian meteorites have suffered shock pressures around 5–20 GPa (nakhlites) and 30–45 GPa (shergottites) (Fritz et al. 2005) whereas 90% of ordinary chondrites have been shocked to above 5 GPa (Schulze and Stöffler 1997). In contrast, 65% of carbonaceous chondrites have not suffered peak pressures above 5 GPa (Scott et al. 1992).

Shock waves can modify the magnetic record of meteorites in at least three ways (Fig. 2). First, they can partially or completely erase the pre-shock remanent magnetization (e.g., Cisowski et al. 1975; Cisowski and Fuller 1978; Gattacceca et al. 2006; Gilder et al. 2006; Bezaeva et al. 2007). In the presence of an ambient field, they can lead to the acquisition of shock remanent magnetization (e.g., Doell et al. 1970; Wasilewski 1973; Pohl et al. 1975; Cisowski et al. 1975, 1976; Cisowski and Fuller 1978; Pohl and Eckstaller 1981; Gattacceca et al. 2008a; Bezaeva et al. 2009). Finally, above 5–10 GPa, shocks (and even quasistatic pressure) can also permanently modify the intrinsic magnetic properties of rocks, including saturation remanent magnetization, coercivity, susceptibility, and anisotropy of susceptibility and remanence (Pohl and Eckstaller 1981;

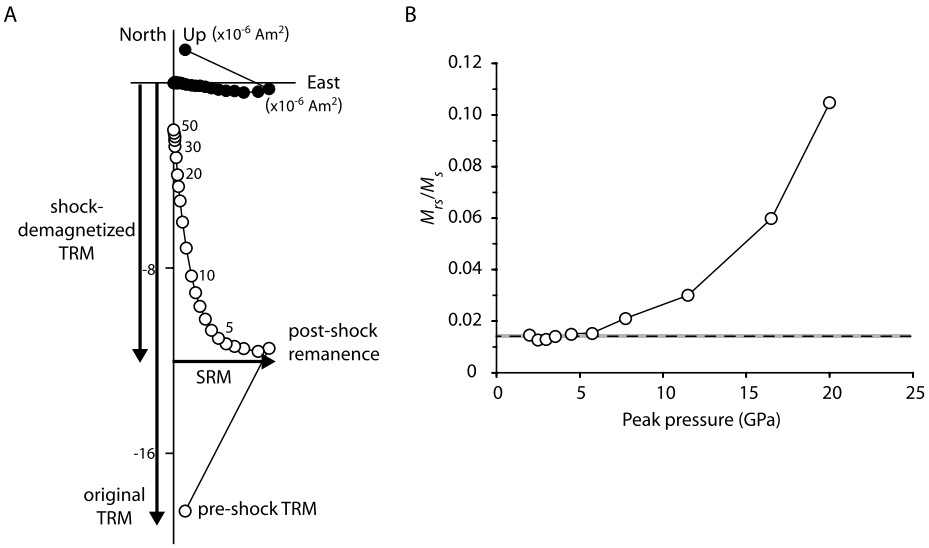

Fig. 2 Effects of shock on remanent magnetization and rock magnetic properties. **A** Orthogonal demagnetization plot showing simultaneous shock demagnetization and remagnetization of a basalt sample. *Open and closed symbols* represent projections of the endpoint of the magnetization vector on vertical and horizontal planes, respectively. The sample, originally carrying a thermoremanent magnetization (TRM) acquired in a 100 μT vertical downward-pointing field, was shocked with a pulsed laser to peak pressures of ∼1 GPa in a 100 μT field horizontal eastward-pointing field. Subsequent AF demagnetization (selected steps shown in mT) isolated two overlapping components of magnetization: a newly acquired SRM superimposed on the partially demagnetized TRM (Gattacceca, unpublished data). **B** Modification of rock magnetic properties of a microdiorite sample shocked with a high-power explosive (M_{rs}: remanent magnetization following exposure to saturating field, M_s: saturation magnetization). *Dashed line* is the mean value for unshocked samples (*grey band* = one s.d.). Adapted from Gattacceca et al. (2007)

Gattacceca et al. 2007; Louzada et al. 2007, 2009; Gilder and Le Goff 2008; Nishioka et al. 2007; Funaki and Syono 2008).

The sensitivity to pressure demagnetization and remagnetization is controlled by the magnetic mineralogy (Kletetschka et al. 2004b; Bezaeva et al. 2007; Louzada et al. 2009). Pyrrhotite has a magnetic phase transition at ∼2.8 GPa (Rochette et al. 2003a), meaning that pyrrhotite-bearing meteorites shocked above this pressures may have lost all or much of the record of their pre-shock remanent magnetization (Rochette et al. 2001; Louzada et al. 2007). This is particularly crucial for basaltic shergottites and Rumuruti chondrites in which pyrrhotite is the main remanence carrier (Rochette et al. 2008, 2009a) and which have generally been shocked to pressures in excess of 5 GPa (Kallemeyn et al. 1996; Fritz et al. 2005). It is also relevant for carbonaceous chondrites that contain pyrrhotite (e.g., Allende) along with FeNi metal and magnetite.

Magnetite is also strongly affected by pressures in the order of a few GPa (Gilder and Le Goff 2008; Gilder et al. 2006; Bezaeva et al. 2009). Presently, the effects of shock on the magnetization and magnetic properties of FeNi metal alloys are still poorly understood (Pohl and Eckstaller 1981). Recent studies have found that the sensitivity to shock decreases from kamacite to taenite to tetrataenite, which correlates with the relative coercivities of these minerals (Bezaeva et al. 2009). FeNi metal may have a phase transition at ∼10–13 GPa (Wasilewski 1973, 1976; Dickinson and Wasilewski 2000).

As a consequence, it appears that the magnetic remanence of shocked meteorites is often unlikely to predate the last major shock event. The major difficulty with this is that nearly all known petrographic shock barometers can only distinguish past shock events with pressures above 4–5 GPa (e.g., Bischoff and Stoffler 1992; Scott et al. 1992). Shock events below 5 GPa leave almost no petrographic imprints but nevertheless can seriously disturb remanent magnetization. In metal-bearing meteorites, anisotropy of magnetic susceptibility is a sensitive shock-induced strain indicator (Gattacceca et al. 2005), but there is a crucial need for developing low-shock quantitative diagnostic techniques in the 0–5 GPa range.

Despite these complications, shocked meteorites should not be immediately rejected for paleomagnetic studies because shock magnetization and demagnetization processes are becoming increasingly well understood. It is now clear that shock remanent magnetization is usually acquired parallel to the ambient field at the time of shock with an intensity proportional to this ambient field (Pohl et al. 1975; Gattacceca et al. 2008a), making it a good recorder of the paleomagnetic field at the time of the last major impact. The main remaining difficulty is that the ambient field at the time of impact may be transiently produced (Crawford and Schultz 1988, 1991, 1993, 1999; Srnka 1977; Doell et al. 1970) or amplified (Hide 1972; Hood 1987; Hood and Artemieva 2008) by the impact itself, therefore making the interpretation of SRM in meteorites a complex topic. On the other hand, for shock pressures above ~40 GPa, the shock-induced temperature increase (Bischoff and Stoffler 1992; Artemieva and Ivanov 2004) is usually high enough to impart a thermoremanent magnetization (TRM) to the rock during slow cooling from post-shock temperatures of ~400–1100°C. The relatively slow thermoremanent magnetization (TRM) acquisition process for such samples is highly unlikely to be magnetized by transient impact-generated fields, which are estimated to last <1 d for the largest basin-forming impacts (Hood and Artemieva 2008) and <100 s for craters <100 km in diameter (Srnka 1977; Crawford and Schultz 1999). For lower shock pressures, localized heterogeneous shock-heating may also be responsible for the acquisition of a TRM, as has been invoked for Martian meteorite ALH 84001 (Weiss et al. 2008b).

In view of the complexity of these shock effects, the main conclusion is that careful selection of unshocked meteorites is the only way to ascertain a possible primary origin of the remanent magnetization (e.g., Weiss et al. 2008a), but that highly shocked and thermally processed samples can play an important subsidiary role in constraining planetary paleomagnetism.

2.4 Inverse Thermoremanent Magnetization

The cubic iron oxide minerals of the magnetite-ulvöspinel series (commonly referred to collectively as titanomagnetite) are important ferromagnetic minerals in carbonaceous chondrites (Herndon et al. 1976; Rochette et al. 2008), angrites (Weiss et al. 2008a), and some Martian meteorites (Rochette et al. 2009a). Nearly stoichiometric magnetite ($Fe_{3-x}Z_xO_4$ with $x < 0.01$–0.02 for a wide range of impurities Z) undergoes two transitions at low temperatures: (1) a magnetic transition at ~130 K when the first magnetocrystalline anisotropy constant passes through zero and (2) a first-order phase transition at ~119 K to a low-temperature monoclinic structure. Nonstoichiometric magnetite will undergo the first transition (usually at a lower temperature that depends on the nature and amount of impurity) but not the second. A number of authors have shown that as a rock warms through each of these transitions in the presence of a magnetic field, it can become magnetized. This "inverse thermoremanent magnetization" (ITRM) could potentially overprint a primary remanence (Dunlop 2006). It has even been suggested that meteorites could be remagnetized

by the Earth's magnetic field as they warm up from space temperatures during atmospheric entry.

Meteorites and asteroids will be typically at an equilibrium temperature set by incoming and reradiated solar insolation. For a fast rotating object, the global average equilibrium temperature is given by $T_{eq} = [F_{Sun}(1-A)/4\varepsilon\sigma a_{AU}^2]^{1/4}$ where F_{Sun} is the solar constant (flux at 1 AU), A is the geometric albedo, a_{AU} is the semimajor axis in AU, ε is the emissivity, σ is Stefan–Boltzmann's constant (de Pater and Lissauer 2001). The latitude (λ) dependent equilibrium temperature for a fast rotating object is $T_{eq,l}(\lambda) = T_{eq}[4\cos(\lambda)/\pi]^{1/4}$. For zero albedo and unit emissivity, this means that even at the outer edge of the entire asteroid belt at 3.5 AU, fast rotators have $T_{eq} \sim 150$ K, which is still well above magnetite's isotropic point. However poleward of $\sim$60° latitude in this region of the solar system, temperatures will be below 130 K. Furthermore, samples from the outer solar system, the unilluminated sides of slowly rotating asteroids, and permanently shadowed craters will also be at temperatures below 130 K. On the other hand, because the transfer of meteorites from the asteroid belt and beyond is a gradual process initiated by resonant interactions with the giant planets, the delivery process typically takes millions of years, with even the fastest known scenarios requiring $\sim$100,000 years (Nesvorný et al. 2007). Therefore, by the time any meteoroid reaches the Earth's field, it should long have warmed up through the isotropic point and so will not have acquired an ITRM. The chances of encountering a strong field along the way to Earth are remote given the low number density of objects in the solar system. The most likely effects of warming through these transitions is therefore demagnetization of pre-existing NRM, which would then tend to lead to underestimates of the true paleointensity and hardening of NRM.

2.5 Unusual Ferromagnetic Minerals and Magnetization Acquisition Mechanisms

Two related difficulties with interpreting the meteorite paleomagnetic record are the presence of ferromagnetic minerals with unfamiliar magnetic properties and poorly understood nonthermal NRM acquisition mechanisms (Rochette et al. 2009b). The reduced oxidation state of many classes of meteorites reflects the formation of FeNi alloys (predominantly with the crystallographic structure of α kamacite, but also γ taenite, γ'' tetrataenite, and γ' awaruite) and, in the most reduced meteorites (ureilites, aubrites and enstatite chondrites), suessite [$(Fe, Ni)_3Si$], schreibersite [$(Fe, Ni)_3P$], and cohenite [$(Fe, Ni)_3C$]. The magnetic properties of the latter three phases are not well known.

Another problem is that, depending on the cooling rate and Ni-content, FeNi can form a variety of metastable ferromagnetic phases whose magnetic properties are not only mostly unknown but which acquire NRM via poorly understood phase-transformation thermochemical mechanisms (for a review, see Garrick-Bethell and Weiss 2009). For bulk compositions with >3% Ni and slow cooling, kamacite and taenite continually equilibrate below kamacite's Curie temperature during cooling to produce a phase-transformation CRM in the kamacite. It is not known if such a remanence mechanism retains a memory of TRM acquired at earlier equilibrium states (Dunlop and Ozdemir 1997). For fast cooling, there are six different possible composition-invariant transformations in the Fe-Ni system (Wilson 1994) including the common meteoritic mineral martensite (α_2Fe). How any of these phases magnetize is very poorly understood (e.g., Wasilewski 1974a, 1974b; Wasilewski et al. 2002).

For high-Ni (>$\sim$50%) metal, tetrataenite and awaruite form by low-temperature atomic ordering of taenite during cooling of the parent body below 320°C and $\sim$500°C, respectively. Tetrataenite, first described in meteorites (Clarke and Scott 1980), is not known in terrestrial rocks because its formation requires high nickel contents and usu-

ally extremely slow cooling (<∼1–100°C/Ma). Its extremely high coercivity compared to taenite and kamacite (Nagata and Funaki 1982, 1987; Nagata 1983; Wasilewski 1988; Nagata and Carleton 1989; Gattacceca et al. 2003) makes it a possible stable carrier of early solar system remanent magnetization. Indeed, LL chondrites that are rich in tetrataenite have much more stable NRM than tetrataenite-poor H and L chondrites (Gattacceca and Rochette 2004). However the relationship of tetrataenite's NRM with that of the precursor taenite is largely unknown, which makes the interpretation of tetrataenite-carried remanent magnetization tentative. In fact, tetrataenite formation is a candidate explanation for the small-scale randomness of NRM directions in some meteorites (Wasilewski et al. 2002; Gattacceca et al. 2003).

2.6 Weathering

Meteorites are subjected to low-temperature aqueous alteration after arrival at the Earth's surface. Metal and sulfide phases are rapidly altered to a variety of oxides and oxyhydroxides, while primary oxides like magnetite are more slowly altered to oxyhydroxides and other oxides like maghemite and hematite. The resulting destruction of primary ferromagnetic minerals and the production of new ferromagnetic minerals in the Earth's field can dramatically overprint preterrestrial NRM in meteorites.

Hot desert finds (i.e., from the Sahara and Arabia) and Antarctic meteorites exhibit different styles of weathering that reflects their discovery locations. Hot desert meteorites, which typically have terrestrial ages of 10–20 thousand years (ka) and rarely survive beyond 50 ka, generally weather much more rapidly than those from Antarctica (the latter have mean residence time of finds of $\sim 10^5$ years, with some finds as old as ∼2 Ma) (Bland et al. 2000, 2006). As a result, hot desert finds have comparatively smaller abundances of metal and troilite and larger abundances of iron oxides and iron oxyhydroxides. Mössbauer spectroscopy (Bland et al. 1998) and electron microscopy studies (Al-Kathiri et al. 2005) have generally revealed two major classes of magnetic weathering minerals: superparamagnetic goethite and paramagnetic phases including akaganéite and lepidocrocite, and ferromagnetic phases including magnetite, maghemite, and hematite. Magnetite is rare and akaganéite is common in Antarctic meteorites, while the opposite is true for hot desert meteorites. Metal will typically first alter to akaganéite or, where dissolution is very rapid, to magnetite. Pyrrhotite, troilite and silicates may first convert to ferrihydrite. These products may then ultimately transition to goethite, maghemite, hematite and lepidocrocite, with in some cases magnetite remaining as a metastable end product (Bland et al. 2006).

Weathering of metal-bearing meteorites is extremely rapid, particularly in hot desert environments (Fig. 3). Several recent studies of desert weathering of ordinary chondrites meteorites found that a large fraction of the metal (tens of percent) is oxidized within just a few hundred to a few thousand years after landing (Al-Kathiri et al. 2005; Al-Rawas et al. 2007; Bland et al. 1996, 1998; Buchwald and Clarke 1989; Lee and Bland 2004; Lee et al. 2006), with essentially 100% of the metal in meteorites from Oman destroyed within just 20 ka. These studies show that pyrrhotite and troilite are more resistant than metal, taenite is more resistant than kamacite, and magnetite and crystalline silicates (including olivine) are more resistant than both metal and sulfides (Gooding 1986; Al-Kathiri et al. 2005; Lee and Bland 2004). Therefore, most meteorites are far more susceptible to weathering remagnetization than typical magnetite-bearing terrestrial rocks; meteoritic silicate phases can be extremely fresh and show no signs of alteration while the metal can be thoroughly weathered.

Rock magnetic studies reflect the destruction of primary ferromagnetic phases in finds (Rochette et al. 2003b, 2008, 2009a). Progressive weathering often leads to a decrease in

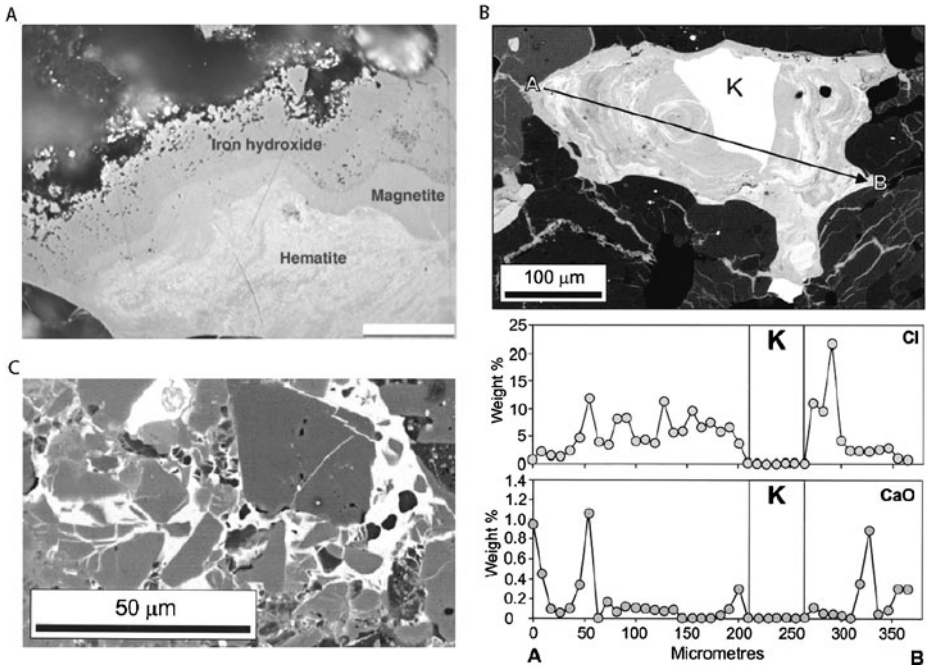

Fig. 3 Weathering of metal and sulfides in chondrites. **A** Backscattered scanning electron microscopy (BSEM) image of hot desert meteorite Al Huqf 010 showing iron oxide and oxyhydroxide weathering products of troilite and kamacite. After (Al-Kathiri et al. 2005). **B** BSEM image of partially weathered kamacite (K) from hot desert meteorite Daraj 014. Concentric layers of weathering products mantle a core of fresh metal. Note light-colored veins of oxyhydroxides within surrounding silicates. Cl and Ca concentrations along the transect **A**–**B**, shown in *lower two panels*, are enhanced in the altered zone and its margins. After (Lee and Bland 2004). **C** BSEM image of weathering-induced brecciation of Antarctic meteorite ALHA 77002. Clasts of olivine, orthopyroxene and feldspar are cemented by Fe-silicate (*lower left hand side*) and a fine-scale intergrowth of iron silicate with iron oxide and oxyhydroxides (*middle right hand side*). After (Lee and Bland 2004)

susceptibility as metal is converted to less magnetic oxides and an increase in NRM as the new phases acquire a crystallization remanent magnetization in the Earth's field (Guskova 1988). This increase in NRM has also been observed in artificial weathering experiments in the laboratory (Kohout et al. 2004).

A robust method for determining whether a meteorite has been remagnetized since arrival on Earth by weathering, viscous magnetization acquired in the Earth's field (e.g., Nagata 1981; Weiss et al. 2008a; Brecher and Arrhenius 1974), or hand magnets (see Sect. 2.7) is the fusion crust baked contact test (Butler 1972; Sugiura and Strangway 1983; Nagata and Funaki 1983; Weiss et al. 2000, 2002, 2008a, 2008b). The basis of this technique is that the fusion crust, the <1 mm thick melted exterior rind typically acquired as a result of heating during passage through Earth's atmosphere, and the immediately adjacent baked interior acquire an approximately unidirectional thermoremanent magnetization (TRM) in Earth's field (Nagata and Sugiura 1977; Nagata 1979d; Weiss et al. 2000, 2002, 2008b). Because the thermal remagnetization zone from atmospheric passage typically only penetrates less than several mm into the interior of stony meteorites, NRM directions of deep interior subsamples should be different from fusion crusted subsamples if there has been no process that has unidirectionally magnetized the en-

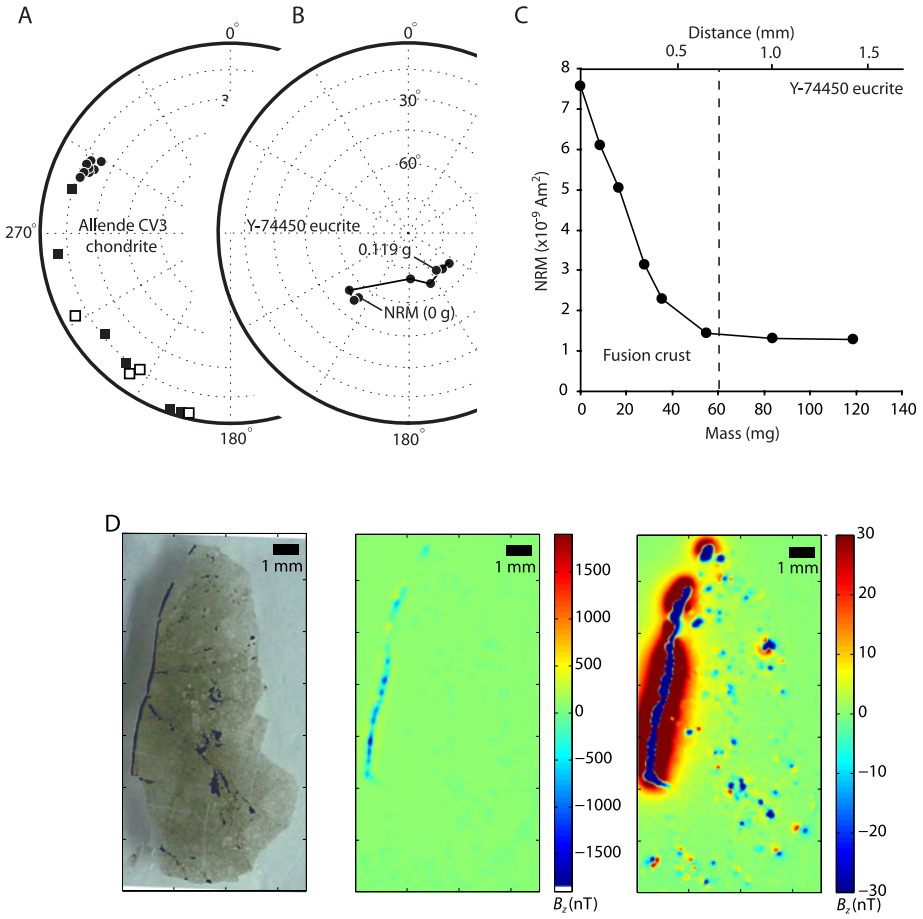

Fig. 4 Fusion crust baked contact for meteorite paleomagnetism. **A** Equal area projection showing directions of NRM of subsamples of Allende meteorite. *Circles* = subsamples from meteorite interior. *Squares* = subsamples from fusion crusted exterior. Adapted from Butler (1972). **B** Equal area projection showing NRM direction of a chip from the Y-74550 eucrite. Fusion crust was progressively scraped off the sample, with the NRM of the remaining chip measured after each scraping step. The NRM direction of the chip changed continuously until the fusion crust was fully removed (after sixth scraping step). Adapted from Nagata (1979d). **C** NRM of Y-74550 chip shown in **B** as a function of cumulative removed mass and depth of removed material. *Dashed line* shows depth of the fusion crust. Adapted from Nagata (1979d). **D** NRM field of martian meteorite ALH 84001. *Left*: Reflected light photograph of 30 μm thin section 227b,2 showing pyroxene (*light brown*), fusion crust *along left side* (*black*) and chromite (*black interior grains*). *Middle*: Vertical component of the NRM field as measured 140 μm above the sample. Positive (out-of-the-page) fields are *red and yellow* and negative (into-the-page) fields are *blue*. The field is dominated by the fusion crust magnetized approximately downward. *Right*: Same as middle except with color scale stretched to show weak, heterogeneously oriented magnetization in the meteorite interior. Adapted from Weiss et al. (2008b).

tire meteorite since its arrival on Earth (Fig. 4). In conducting this test, ratios of NRM/IRM should be measured in concert with measuring NRM directions, because magnets (Sect. 2.7) will often only remagnetize the outer several cm of large meteorites (e.g., Fig. S1B of Weiss et al. 2008a). The proximity of the magnets to the outer portion of a meteorite will produce NRM directions in exterior subsamples that are divergent from deep interior subsamples

and give the appearance of a positive baked contact test. High ($>\sim$10%) NRM/IRM ratios in exterior samples can be used to discard such false positives.

2.7 Hand Magnets and Secondary IRM

Even if a meteorite has been demonstrated to not be completely remagnetized by terrestrial weathering, it may still not contain a pre-terrestrial paleomagnetic record as a result of contamination by IRM. Unfortunately, one of the most common techniques for establishing the extraterrestrial nature and meteorite classification of a find is to quickly estimate its metal content by application of a hand magnet. Typical refrigerator magnets produce surface fields of several tens of mT, while rare earth magnets (in wide use among meteorite hunters and dealers) commonly produce surface fields of hundreds of mT. Most meteorites found in hot deserts (e.g., Acfer, Dar al Gani, Dhofar, Northwest Africa, Sahara, meteorites) as well as many meteorite falls have been magnetically contaminated with rare earth magnets (Fig. 5).

Because ferromagnetic minerals in meteorites typically have maximum coercivities ranging from 300 mT (magnetite) to $\sim$1 T (metal), rare earth magnets (but not common magnets) will destroy most of the NRM at the contact point immediately upon application of the magnet. As the magnet is withdrawn, the contact point will experience a field that changes in direction and weakens in time as the curved fields of the increasingly distant magnet sweep through the point. This blocks different coercivity fractions in different directions, producing a NRM that demagnetizes in curvilinear fashion during AF treatment (Fig. 5). Adjacent locations in the meteorite will experience a different field history and so will be magnetized in a different direction. Therefore the magnet IRM in a meteorite is expected to be spatially nonuniform in direction (as well as in magnitude) throughout the meteorite.

Because of the rapid falloff of fields with distance from hand magnets (proportional to r^{-2} to r^{-3} at the scale of meteorite hand samples), parts of the meteorite that are several cm away from the contact point will retain a high coercivity fraction of their NRM, with the deep interior ($>$10 cm) nearly unaffected by magnet overprints. Therefore, as discussed in Sect. 2.6, for large ($>\sim$20 cm diameter) meteorite fragments, AF demagnetization of mutually oriented subsamples from a range of depths can be used to isolate NRM in the deep interior of the meteorite (see Fig. S1b of Weiss et al. 2008a; numbers in parentheses next to each subsample in this figure give distance in mm from the fusion crusted exterior). Note that thermal demagnetization, which does not activate the same grain distribution as that affected by an IRM, is *not* very effective at removing IRM overprints (e.g., Lawrence et al. 2008). In the "magnet contact test", subsamples should have more intense NRM due to increasingly strong IRM overprints as the magnet contact point is approached; the unblocking coercivity of this IRM should similarly increase. In the magnet remagnetized zone, the NRM will be spatially nonuniform and exhibit curvilinear components during AF demagnetization (e.g., Fig. 5). The deep interior fraction of a meteorite unaffected by the IRM which contains a primary TRM will have an NRM that is usually far from saturation, spatially uniform in direction, and composed of linear magnetization components that are oriented differently from much of the magnet zone.

3 Paleomagnetic Records in Chondrites

We now turn to the actual paleomagnetic records of meteorites. We begin with the most primitive samples, chondrites. Chondrites are polymict breccias of early solar system solids (refractory inclusions, chondrules, and matrix) that lithified on early formed planetesimals.

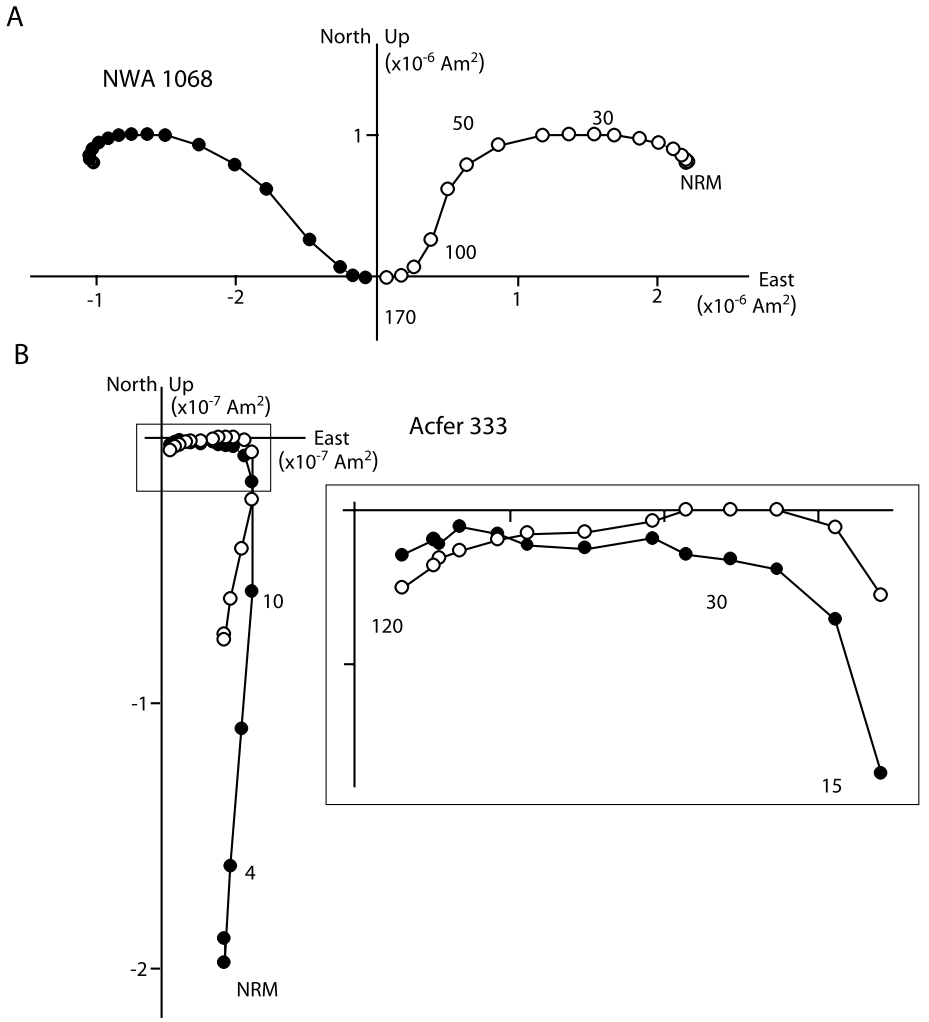

Fig. 5 Orthogonal demagnetization plot showing AF demagnetization of the NRM of meteorites previously remagnetized by exposure to artificial strong fields (hand magnets). Open and closed symbols represent projections of the magnetization vector on vertical and horizontal planes, respectively. Selected AF demagnetization steps are labeled in mT. **A** Shergottite NWA 1068 has been totally remagnetized by strong fields and exhibits the corresponding typical curved demagnetization pattern. It has ratios of NRM to saturation IRM (sIRM) of ∼0.11 and derivatives of NRM/sIRM with respect to AF step (known as REM′) ∼ 0.1 throughout the whole demagnetization process. **B** CO chondrite Acfer 333 has been partially remagnetized by a strong field as indicated by REM′ ∼ 0.1 in the 0 to 15 mT AF range. However, a high coercivity magnetization component isolated between 30 and 120 mT was not reset by magnet exposure, as indicated by REM′ $\sim 2 \times 10^{-3}$ over this AF range. Adapted from Gattacceca and Rochette (2004)

Although they have never experienced subsequent melting, their constituents experienced varying amounts of aqueous alteration and thermal metamorphism in the solar nebular and/or on their parent planetesimals. Because chondrites sample bodies that have never experienced total melting, their magnetic record remains less well understood relative to

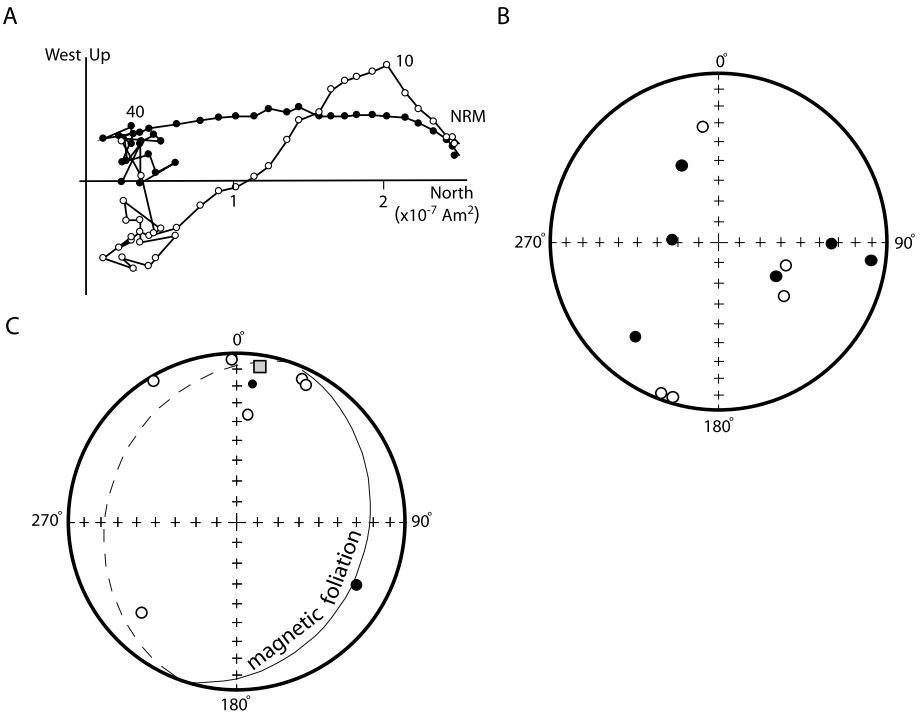

Fig. 6 NRM in the interior of the Bensour LL6 meteorite. **A** Orthogonal demagnetization plot of a ∼ 0.4 g sample of Bensour. Open and solid symbols represent projections of the endpoint of the magnetization vector on vertical and horizontal planes, respectively. Selected demagnetization steps are listed in mT. At least three components of magnetization can be distinguished. **B** Equal area stereographic projection of the medium coercivity (10 to 40 mT) components (corrected for anisotropy of remanence) of 11 mutually oriented samples of Bensour. **C** Equal area stereographic projection of the low coercivity components (NRM to 10 mT) of 8 mutually oriented samples of Bensour. *The grey box* is the magnetic lineation and *the great circle* is the magnetic foliation as determined by anisotropy of magnetic susceptibility and remanence. Adapted from Gattacceca et al. (2003)

igneous meteorites (Sect. 4). A summary of previous paleomagnetic analyses of ordinary and non-ordinary chondrites is given in Tables 1 and 2.

3.1 Ordinary Chondrites

Ordinary chondrites, the most common type of meteorites, have been the target of a large number of paleomagnetic studies starting with Lovering (1959) and Stacey and Lovering (1959). Although most early studies concluded that ordinary chondrites had recorded dynamo-generated or solar extraterrestrial magnetic fields (Stacey and Lovering 1959; Stacey et al. 1961; Lovering 1962), it is now clear that the interpretation of the remanent magnetization of these meteorites is likely to have been substantially altered since formation by subsequent thermal, shock, and low-temperature recrystallization processes.

A major difficulty for studying ordinary chondrites is the low coercivity of their main constituent ferromagnetic phases, multidomain kamacite and taenite. This is a key reason why the NRMs of most H and L chondrites exhibit erratic changes in direction and intensity under AF or thermal demagnetization (Brecher and Ranganayaki 1975; Brecher et al. 1977;

Table 1 Summary of previous paleomagnetic studies of ordinary chondrites. All names and classifications are as listed in the Meteoritical Bulletin Database. Other unofficial names are listed in parentheses. Abstracts and unpublished manuscripts were generally excluded unless they were the sole reference for a given meteorite. Numbers following group identification give petrologic type (Hutchison 2004). The extensive NRM measurements (no demagnetization) of Pochtarev and Guskova (1962), Guskova (1969, 1970) are not listed here

Name	Group	References
ALHA76008 (ALH 768)	H6	Westphal (1986)
Achilles	H5	Larson et al. (1973)
Allegan	H5	Larson et al. (1973)
Avanhandava	H4	Kohout et al. (2006)
Barbotan	H5	Brecher and Leung (1979)
Bath	H4	Westphal and Whitechurch (1983), Kukkonen and Pesonen (1983), Westphal (1986)
Borodino	H5	Guskova (1963)
Brownfield (1937)	H3	Brecher and Leung (1979)
Burdett	H5	Brecher and Leung (1979)
Cavour	H6	Brecher and Leung (1979)
Chamberlin	H5	Kukkonen and Pesonen (1983)
Clovis	H3	Kukkonen and Pesonen (1983)
Farley	H5	Brecher and Leung (1979)
Fleming	H3	Pesonen et al. (1993)
Forest City	H5	Kukkonen and Pesonen (1983)
Gilgoin (Gilgoin Station)	H5	Brecher and Leung (1979)
Gladstone	H4	Weaving (1962a)
Gorlovka	H3	Guskova (1982a)
Hessle	H5	Kukkonen and Pesonen (1983)
Holyoke	H4	Brecher and Leung (1979)
Horace	H5	Weaving (1962a)
Hugoton	H5	Kukkonen and Pesonen (1983)
Indio Rico	H6	Westphal and Whitechurch (1983)
Kargapole	H4	Guskova (1983, 1988)
Kernouve (Clegueric)	H6	Weaving (1962a)
Kesen (Kessen)	H4	Nagata and Sugiura (1977), Sugiura (1977), Kukkonen and Pesonen (1983)
Lancon	H6	Brecher and Ranganayaki (1975)
Leighton	H5	Larson et al. (1973)
Markovka	H4	Guskova (1988)
Metsäkylä	H4	Kukkonen and Pesonen (1983)
Mooresfort	H5	Westphal and Whitechurch (1983)
Morland	H6	Larson et al. (1973)
Mount Browne	H6	Stacey and Lovering (1959), Stacey et al. (1961)
Oakley Stone	H6	Westphal (1986), Westphal and Whitechurch (1983)

Table 1 (*Continued*)

Name	Group	References
Ochansk	H4	Westphal and Whitechurch (1983), Guskova (1963); Brecher and Ranganayaki (1975), Guskova (1976a), Brecher and Leung (1979)
Orlovka	H5	Guskova and Pochtarev (1969)
Petropavlovka	H4	Guskova (1983)
Plainview (1917)	H5	Wasilewski and Dickinson (2000), Wasilewski et al. (2002)
Prairie Dog Creek	H3	Westphal (1986), Westphal and Whitechurch (1983)
Pultusk	H5	Guskova (1963), Guskova (1976a), Brecher and Leung (1979) Westphal and Whitechurch (1983), Westphal (1986), Guskova (1965a)
Quenggouk	H4	Brecher and Ranganayaki (1975)
Raguli	H3	Guskova (1988)
Richardton	H5	Yu et al. (2009)
Rose City	H5	Brecher and Ranganayaki (1975)
Saline	H5	Brecher and Leung (1979)
Seminole	H4	Nagata and Sugiura (1977)
Severny Kolchim	H3	Guskova (1988)
Ställdalen	H5	Guskova (1963), Kukkonen and Pesonen (1983)
Sverdlovsk	H4/5	Guskova (1988)
Tysnes Island	H4	Brecher and Ranganayaki (1975)
Vernon County	H6	Kukkonen and Pesonen (1983)
Y-694	H6	Nagata (1979c)
Y-7301	H5/6	Nagata and Sugiura (1977), Nagata (1979c)
Y-7312	H5	Sugiura (1977)
Y-74014	H6	Westphal (1986)
Y-74371	H4	Sugiura (1977), Westphal (1986)
Y-74640	H6	Westphal (1986)
Y-74647	H5	Sugiura (1977), Nagata (1979c), Westphal (1986)
Yatoor (Nellore)	H5	Weaving (1962a), Guskova (1983)
Yonozu	H4/5	Nagata and Sugiura (1977)
Zhovtnevyi	H6	Guskova (1963, 1976a)
ALHA76009 (ALH 769)	L6	Nagata (1979c), Funaki et al. (1981)
ALHA77260	L3	Nagata and Funaki (1982), Nagata (1983)
Alfianello	L6	Kukkonen and Pesonen (1983), Gattacceca and Rochette (2004)
Andover	L6	Brecher and Ranganayaki (1975)
Aumale	L6	Brecher and Ranganayaki (1975)
Bachmut	L6	Guskova (1983)
Bakhardok	L6	Guskova (1988)
Bald Mountain	L4	Brecher and Ranganayaki (1975)
Barratta	L4	Stacey et al. (1961), Kukkonen and Pesonen (1983)
Bjurböle	L/LL4	Stacey et al. (1961), Brecher and Ranganayaki (1975), Sugiura and Strangway (1982), Kukkonen and Pesonen (1983), Wasilewski and Dickinson (2000), Wasilewski et al. (2002), Acton et al. (2007)

Table 1 (*Continued*)

Name	Group	References
Bluff (a or b?)	L5 or L4?	Guskova (1982a), Kukkonen and Pesonen (1983)
Brewster	L6	Weaving (1962a, 1962b)
Bruderheim	L6	Larson et al. (1973), Kukkonen and Pesonen (1983)
Buschhof	L6	Brecher and Ranganayaki (1975), Kukkonen and Pesonen (1983)
Cabezo de Mayo	L/LL6	Brecher and Ranganayaki (1975)
Calliham	L6	Larson et al. (1973)
Chateau-Renard	L6	Guskova (1963)
Dalgety Downs	L4	Nagata and Sugiura (1977)
Elenovka	L5	Guskova and Pochtarev (1969)
Ergheo	L5	Kukkonen and Pesonen (1983)
Farmington	L5	Stacey et al. (1961), Larson et al. (1973), Guskova (1982a)
FRO 01064	L6	Gattacceca and Rochette (2004)
FRO 01097	L6	Gattacceca and Rochette (2004)
Fukutomi	L5	Nagata and Sugiura (1977)
Gifu (Mino)	L6	Sugiura (1977), Nagata and Sugiura (1977)
Hallingeberg	L3	Gattacceca and Rochette (2004)
Holbrook	L/LL6	Kukkonen and Pesonen (1983)
Homestead	L5	Stacey and Lovering (1959), Stacey et al. (1961)
Julesburg	L3	Gattacceca and Rochette (2004)
Kunashak	L6	Guskova (1976a)
L'Aigle	L6	Guskova (1963, 1976a)
La Lande	L5	Larson et al. (1973)
Ladder Creek	L6	Gattacceca and Rochette (2004)
Leedey	L6	Gattacceca and Rochette (2004)
Long Island	L6	Gattacceca and Rochette (2004)
Marion (Iowa)	L6	Guskova (1983)
McKinney	L4	Guskova (1982a)
Melrose	L5	Larson et al. (1973)
Mezö-Madaras	L3	Guskova and Pochtarev (1969), Sugiura and Strangway (1982)
Mocs	L5-6	Guskova (1963)
Monte Milone	L5	Gattacceca and Rochette (2004)
Ness County	L6?	Larson et al. (1973)
Ozernoe	L6	Guskova (1988)
Pavlograd (Mordvinovka)	L6	Guskova (1963, 1976a)
Pervomaisky	L6	Guskova and Pochtarev (1969)
Potter	L6	Larson et al. (1973)
Rakovka	L6	Guskova (1963, 1976a)
Salla	L6	Kukkonen and Pesonen (1983)
St. Michel	L6	Kukkonen and Pesonen (1983)
Saratov	L4	Guskova (1963, 1976a)
Sevrukovo	L5	Guskova (1963)
Slobodka	L4	Guskova (1963)
Tadjera	L5	Brecher and Ranganayaki (1975)

Table 1 (*Continued*)

Name	Group	References
Tarbagatai	L5	Guskova and Pochtarev (1969), Guskova (1976a)
Tathlith	L6	Gattacceca and Rochette (2004)
Tsarev	L5	Guskova (1982b, 1988)
Utrecht	L6	Brecher and Ranganayaki (1975)
Valkeala	L6	Kukkonen and Pesonen (1983)
Y-7304	L6	Sugiura (1977), Nagata (1979c)
Y-7305	L6	Nagata (1979c)
Y-74191	L3	Sugiura (1977), Nagata (1979c, 1979e), Sugiura and Strangway (1982)
Y-74362	L6	Sugiura (1977), Nagata (1979c, 1979d)
Zavetnoe	L6	Guskova (1963)
Zavid	L6	Brecher and Ranganayaki (1975)
ALHA77304	LL3	Nagata et al. (1986)
Appley Bridge	LL6	Larson et al. (1973)
Arcadia	LL6	Larson et al. (1973)
Beeler	LL6	Gattacceca and Rochette (2004)
Bensour	LL6	Gattacceca et al. (2003), Gattacceca and Rochette (2004)
Chainpur	LL3	Wasilewski and Dickinson (2000), Sugiura and Strangway (1982)
Dhurmsala	LL6	Brecher et al. (1977), Kukkonen and Pesonen (1983), Gattacceca and Rochette (2004)
Ensisheim	LL6	Brecher et al. (1977), Kukkonen and Pesonen (1983)
Guidder	LL5	Pesonen et al. (1993), Gattacceca and Rochette (2004)
Hamlet	LL4	Larson et al. (1973)
Jelica	LL6	Brecher and Ranganayaki (1975)
Kelly	LL4	Larson et al. (1973)
Kilabo	LL6	Gattacceca et al. (2003), Gattacceca and Rochette (2004)
Krymka	LL3	Gattacceca and Rochette (2004)
Lake Labyrinth	LL6	Brecher et al. (1977)
Manbhoom	LL6	Kukkonen and Pesonen (1983), Gattacceca and Rochette (2004)
Melnikovo	LL6	Guskova (1988)
Olivenza	LL5	Larson et al. (1973), Brecher et al. (1977), Gattacceca et al. (2003), Gattacceca and Rochette (2004)
Oued el Hadjar	LL6	Gattacceca and Rochette (2004)
Parnallee	LL3	Brecher et al. (1977)
Saint-Séverin	LL6	Brecher and Ranganayaki (1975), Brecher et al. (1977), Sugiura (1977), Nagata and Funaki (1982), Nagata (1983) Nagata et al. (1986)
Soko-Banja	LL4	Brecher and Ranganayaki (1975), Brecher et al. (1977) Kukkonen and Pesonen (1983)
St. Mesmin	LL6	Brecher et al. (1977), Gattacceca and Rochette (2004)
Vavilovka	LL6	Brecher and Ranganayaki (1975)
Y-7307	LL6[a]	Nagata (1979a, 1979b, 1979e)
Y-74160	LL7	Nagata and Funaki (1982), Nagata (1983, 1993)
Y-74442	LL4	Nagata (1979c)
Y-74646	LL6	Nagata (1979c, 1979d)
Krutikha	OC ung.	Guskova (1988)

[a]Identified as a howardite by Nagata (1979a), Miyamoto et al. (1978)

Table 2 Summary of previous paleomagnetic studies of non-ordinary chondrites. All names and classifications are as listed in the Meteoritical Bulletin Database. Other unofficial names are listed in parentheses. Abstracts and unpublished manuscripts were generally excluded unless they were the sole reference for a given meteorite. Numbers following group identification give petrologic type (Hutchison 2004). CV chondrites are assigned to the reduced (CV_{red}), Allende-like oxidized (CV_A), and Bali-like oxidized (CV_B) subgroups (Weisberg et al. 2006) and CB chondrites are assigned to subtypes "a" (large chondrules) and "b" (small chondrules)

Name	Group	References
Enstatite		
Abee	EH4	Brecher and Ranganayaki (1975), Sugiura and Strangway (1981, 1982, 1983) Kukkonen and Pesonen (1983), Guskova (1985, 1987)
Adhi Kot	EH4	Guskova (1985, 1987)
Atlanta	EL5	Guskova (1985, 1987)
Daniel's Kuil	EL6	Guskova (1985, 1987)
Hvittis	EL6	Brecher and Ranganayaki (1975), Kukkonen and Pesonen (1983), Guskova (1985, 1987)
Indarch	EH4	Sugiura and Strangway (1982), Guskova (1985)
Khairpur	EL6	Brecher and Ranganayaki (1975), Guskova (1985, 1987)
Kota–Kota	EH4	Guskova (1985, 1987)
Neuschwanstein	EL6	Kohout et al. (2010)
Pillistfer	EL6	Guskova (1985, 1987)
St. Mark's	EH5	Guskova (1985, 1987)
Y-691 (Y-a)	EH3	Sugiura and Strangway (1982), Nagata et al. (1975), Nagata (1979c) Sugiura (1977)
Carbonaceous		
Bencubbin	CBa	Guskova (1970)
QUE 94411	CBb	Wasilewski (2000)
Ivuna	CI1	Brecher and Arrhenius (1974), Guskova (1976b)
Orgueil	CI1	Banerjee and Hargraves (1971, 1972), Brecher and Arrhenius (1974), Guskova (1976b, 1978), Nagata (1979b, 1979e), Kukkonen and Pesonen (1983)
Karoonda	CK4	Brecher and Arrhenius (1974), Guskova (1976b), Sugiura (1977), Nagata (1979b, 1979e), Acton et al. (2007)
Kobe	CK4	Funaki and Nakamura (2002)
Y-693 (Y-c)	CK4/5	Nagata et al. (1975), Sugiura (1977), Nagata (1979b, 1979c)
Acfer 331	CM2	Gattacceca and Rochette (2004)
Boriskino	CM2	Guskova (1976b)
Cold Bokkeveld	CM2	Banerjee and Hargraves (1971), Larson et al. (1973), Brecher and Arrhenius (1974), Guskova (1976a, 1976b, 1978)
Haripura	CM2	Brecher and Arrhenius (1974), Guskova (1976b)
Kivesvaara	CM2	Pesonen et al. (1993)
Mighei	CM2	Banerjee and Hargraves (1971, 1972), Larson et al. (1973), Brecher and Arrhenius (1974), Guskova (1976b, 1976a, 1978, 1983), Nagata (1979b, 1979e)

Table 2 (*Continued*)

Name	Group	References
Murchison	CM2	Banerjee and Hargraves (1972), Larson et al. (1973), Brecher and Arrhenius (1974), Guskova (1976b, 1983), Kletetschka et al. (2003)
Murray	CM2	Brecher and Arrhenius (1974), Larson et al. (1973), Guskova (1976b, 1983)
Nawapali	CM2	Larson et al. (1973), Guskova (1976b, 1976a, 1978)
Nogoya	CM2	Banerjee and Hargraves (1971), Guskova (1976b, 1976a)
Y-74662	CM2	Nagata (1979b, 1979c), Brecher (1980), Nagata and Funaki (1989), Nagata et al. (1991), Nagata (1993)
Acfer 333	CO3	Gattacceca and Rochette (2004)
Felix	CO3	Larson et al. (1973)
Kainsaz	CO3	Guskova (1976b, 1978), Larson et al. (1973)
Lancé	CO3	Larson et al. (1973)
Ornans	CO3	Pochtarev and Guskova (1962), Guskova (1976b, 1978), Kukkonen and Pesonen (1983)
Warrenton	CO3	Herndon (1974)
Y-81020	CO3	Nagata and Funaki (1989), Nagata et al. (1991), Nagata (1993)
Renazzo	CR2	Guskova (1976b), Larson et al. (1973), Brecher and Arrhenius (1974)
Allende	CV_A3	Butler (1972), Banerjee and Hargraves (1972), Larson et al. (1973), Brecher and Arrhenius (1974), Sugiura (1977), Guskova (1976b), Lanoix et al. (1977), Guskova (1978), Lanoix et al. (1978), Nagata (1979a, 1979b, 1979e), Sugiura et al. (1979), Wasilewski (1981), Wasilewski and Saralker (1981), Nagata and Funaki (1983), Guskova (1983), Sugiura et al. (1985), Nagata and Funaki (1989), Nagata et al. (1991), Nagata (1993), Funaki (2005), Acton et al. (2007), Acton et al. (2007), Carporzen et al. (2009)
Efremovka	$CV_{red}3$	Guskova (1976b)
Grosnaja	CV_B3	Larson et al. (1973), Guskova (1976b)
Kaba	CV_B3	Larson et al. (1973)
Leoville	$CV_{red}3$	Larson et al. (1973), Sugiura (1977), Nagata and Sugiura (1977), Nagata (1979b), Guskova (1983), Nagata et al. (1991)
Mokoia	CV_B3	Stacey et al. (1961), Brecher and Arrhenius (1974)
Vigarano	$CV_{red}3$	Pochtarev and Guskova (1962), Brecher and Arrhenius (1974), Larson et al. (1973), Guskova (1976b)
Coolidge	C4 ung.	Larson et al. (1973), Brecher and Arrhenius (1974)
EET96026	C4-5 ung.	Gattacceca and Rochette (2004)
Tagish Lake	C2 ung.	Gattacceca and Rochette (2004)
Essebi	C2 ung.	Larson et al. (1973)
Rumuruti-like		
A-881988	R4	Gattacceca and Rochette (2004)
ALH 85151	R3	Gattacceca and Rochette (2004)
PCA 91002	R3-6	Gattacceca and Rochette (2004)
PRE 95411	R3	Gattacceca and Rochette (2004)

Brecher and Leung 1979; Funaki et al. 1981; Sugiura and Strangway 1982; Westphal and Whitechurch 1983; Collinson 1987; Morden 1992a; Morden and Collinson 1992; Gattacceca and Rochette 2004). Despite their low coercivity (1.0 ± 0.8 mT, $n = 15$ for H chondrites and 5.3 ± 4.0 mT, $n = 20$ for L chondrites; Gattacceca's unpublished data), H and L chondrites can have high coercivity of remanence (39.4 ± 40.8 mT, $n = 15$ for H chondrites and 153 ± 124 mT, $n = 20$ for L chondrites; Gattacceca's unpublished data), possibly due to a small amount of tetrataenite (Sect. 2.5). LL ordinary chondrites (e.g., Bensour) possess more stable NRM which is mostly carried by abundant tetrataenite (Collinson 1987; Gattacceca et al. 2003) (Fig. 6). Despite its very high coercivity, this mineral is unfortunately not ideally suited for paleomagnetism because it is a secondary phase whose remanent magnetization cannot be simply related to the magnetization of its precursor taenite grain (see Sect. 2.5).

A second major difficulty with studying ordinary chondrites is the small-scale (down to millimeter) heterogeneity of directions of magnetization in L and LL chondrites (Funaki et al. 1981; Collinson 1987; Morden 1992a; Morden and Collinson 1992; Gattacceca et al. 2003). This heterogeneity is observed almost ubiquitously [for some unusual exceptions, see (Sugiura and Strangway 1982; Westphal and Whitechurch 1983)], even in chondrites that suffered parent body metamorphism to temperatures in excess of the Curie temperatures of kamacite, taenite and tetrataenite. This implies that, at least for these equilibrated chondrites, the magnetization postdates parent body thermal metamorphism. The origin of the small-scale scatter of the NRM directions may be from shock-induced brecciation or related to the formation tetrataenite (see Sect. 2.5). In the Bensour LL6 meteorite, a coherent soft magnetization was also isolated blocked by grains with coercivities below 25 mT and oriented parallel to the magnetic lineation (Gattacceca et al. 2003) (Fig. 6). This magnetization may be shock-related or have a viscous origin. The significance of directional homogeneity observed in some H chondrites (Westphal and Whitechurch 1983) is currently unclear.

A third problem is that ordinary chondrite finds should not be considered for paleomagnetic studies because of rapid weathering of metallic phases and associated remagnetization in the Earth magnetic field (e.g., Sect. 2.6). It is noteworthy that for H and L chondrites, finds have much more stable NRM than falls (Gattacceca and Rochette 2004), which is strong evidence that the NRM of finds was acquired as a crystallization remanent magnetization on Earth through weathering.

In conclusion, it is now clear that the high (>10 μT) paleointensities derived from Thellier–Thellier analyses of H, L and LL chondrites in earlier studies (e.g., Nagata and Sugiura 1977; Westphal and Whitechurch 1983; Pesonen et al. 1993) are overestimates and should almost certainly be discarded, as suggested by Westphal (1986), Pesonen et al. (1993). This is because heating of the samples almost invariably led to destabilization of metallic phases (in particular tetrataenite), and also because the laboratory TRM was often matched to a large and soft component of NRM rather than to any smaller stable components. Paleofields in the several μT range or lower (Brecher and Ranganayaki 1975; Brecher et al. 1977; Gattacceca and Rochette 2004) are more realistic.

Progress in the field of ordinary chondrite paleomagnetism should come from additional detailed studies of selected meteorites. Only falls should be studied. Unequilibrated chondrites are the best candidates for investigating possible pre-accretion magnetization, but the unstable magnetization of H and L chondrites and the unknown magnetization mechanism of tetrataenite make this task difficult. In contrast, the study of equilibrated chondrites heated above their Curie temperatures during parent body metamorphism could lead to a new understanding of the small-scale heterogeneous remanent magnetization and the very low (possibly null) field magnetization processes.

3.2 Enstatite (E) Chondrites

Enstatite chondrites are highly reduced, enstatite-rich, olivine-poor meteorites that form two chemical groups: low-Fe (EL) and high-Fe (EH) (Hutchison 2004; Weisberg et al. 2006). Although enstatite chondrites from both groups have been surveyed paleomagnetically (Guskova 1985, 1987; Nagata et al. 1975; Brecher and Ranganayaki 1975; Sugiura and Strangway 1982), by far the best studied is the Abee EH4 meteorite (Brecher and Ranganayaki 1975; Guskova 1985, 1987; Sugiura and Strangway 1981, 1982, 1983). Its NRM is carried by cohenite and kamacite, with cohenite having a more stable component. NRM directions within a given clast are reasonably grouped whereas they widely differ from clast to clast. The NRM directions of matrix subsamples are also grouped. This positive conglomerate test (e.g., Butler 1992) suggests that the magnetization of the clasts predates brecciation of the meteorite and that the clasts have not been heated above the Curie temperature of cohenite (215°C) after brecciation. In view of the shock history of this meteorite, the clast magnetization is probably a TRM acquired after impact melting. Brecciation caused by subsequent impacts randomized the magnetization directions. However, it is difficult to interpret the very high paleointensity values (in the 100 μT–1 mT range) measured by Sugiura and Strangway. New paleomagnetic studies of both high-grade and low-grade enstatite chondrite are clearly necessary.

3.3 Carbonaceous Chondrites

Carbonaceous chondrites offer the most pristine rock record from the preaccretional phase of the early solar system. CI chondrites, although extensively aqueously altered, provide the closest match to the composition of the sun and are therefore thought to be the least chemically fractionated with respect to the bulk solar system (Anders and Grevesse 1989). CV chondrites are less aqueously altered than CI chondrites and contain the largest and most abundant CAIs, the oldest known solar system solids (Brearley and Jones 1998). Several classes of carbonaceous chondrites also contain abundant chondrules, which are collectively the largest mass of preaccretional samples available and which formed from 0–5 Ma after CAIs (Amelin and Krot 2007; Russell et al. 2006). As a result, it has long been recognized that carbonaceous chondrites and their constituents (refractory inclusions and chondrules) potentially offer records of magnetic fields from the solar nebula and the T Tauri Sun.

Of the eight carbonaceous chondrite groups, the CV and CM chondrites are by far the best studied, followed by CO and CI chondrites (Table 2). CK and CR chondrites are unstudied with the exception of a small number of analyses on Karoonda and Renazzo, respectively. Other than an abstract (Wasilewski 2000) and an NRM measurement by Guskova (1970), we are aware of no published studies of CB chondrites. We are aware of no paleomagnetic data at all for CH and CR chondrites.

Given the great petrologic and geochemical complexity of carbonaceous chondrites, detailed paleomagnetic datasets are necessary in order to come to clear conclusions about the magnetic field record. Extensive paleomagnetic data (e.g., analyses of mutually oriented samples, thermal demagnetization, and fusion crust baked contact tests; see Sect. 2) are only available for Allende (CV3). Therefore we will focus on this meteorite and also briefly discuss the much smaller datasets available for Murchison (CM2), Orgueil (CI1) and Karoonda (CK4).

The CV meteorite Allende, a >2000 kg fall in 1969, is the best studied chondrite of any kind and one of the best paleomagnetically studied rocks in history (nearly two dozen studies by ∼9 different groups). Allende and other CV chondrites contain the ferromagnetic phases pyrrhotite, magnetite and metal. Metal is in the form of awaruite ($FeNi_3$)

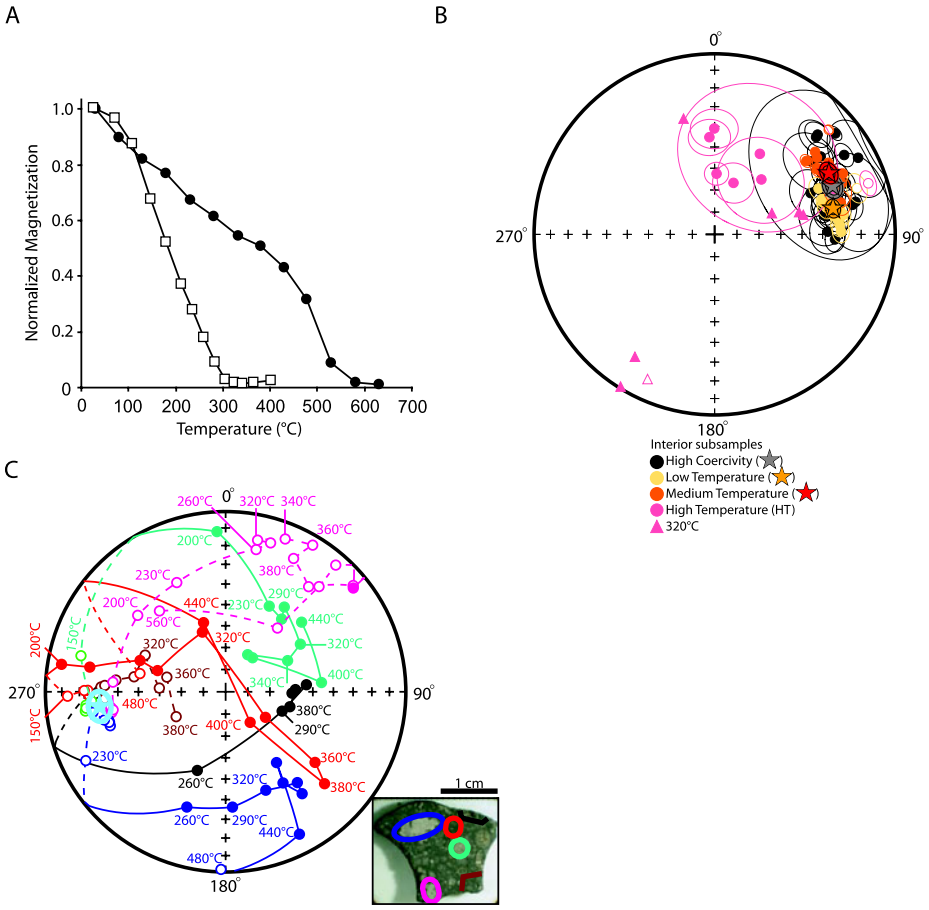

Fig. 7 NRM in the CV carbonaceous chondrite Allende. **A** Remanent magnetization (normalized to the room-temperature value) of bulk samples during thermal demagnetization. *Open symbols* = demagnetization of NRM by Sugiura and Strangway (1985) (their subsample 64). *Closed symbols* = demagnetization of an ARM acquired in a peak ac field of 140 mT and dc bias field of 44 μT by Nagata and Funaki (1983). **B** Equal area stereographic projection showing directions of primary magnetization components of samples from the interior of Allende. *Solid symbols* = lower hemisphere; *open symbols* = upper hemisphere. Ellipsoids are defined as maximum angular deviations associated with the least square fits to sample data. Stars and their ellipsoids represent the average directions and associated 95% confidence intervals. Samples represented by triangles were only thermally demagnetized to 320°C; the directions shown for these are the moments after demagnetization to this temperature (rather than least squares fits). After (Carporzen et al. 2009). **C** Equal area stereographic projection showing directions of NRM during thermal demagnetization of Allende interior subsamples (different parent stone from that shown in **B**). *Inset* shows approximate localizations of subsamples in parent sample prior to extraction. Subsamples are two fine-grained spinel-rich CAIs (*red* and *pink colors*), a porphyritic olivine-pyroxene chondrule (*green color*), an Al-rich chondrule (*blue color*), and two bulk, matrix-rich samples (*brown* and *black colors*). *Light blue* star and ellipsoid are the average NRM direction for the 6 subsamples and associated 95% confidence interval. The bulk samples are demagnetized by <380°C, while CAIs and chondrules retain magnetization directions that move along great circle paths up to ~500°C. After (Carporzen et al. 2009)

in Allende and other oxidized CVs and kamacite in reduced CVs (Krot et al. 1998). Allende shows no evidence of post-accretional shock (above 5 GPa) (Scott et al. 1992), and several fusion crust baked contact tests (e.g., Fig. 4a) have confirmed that it contains highly stable preterrestrial magnetization (Butler 1972; Nagata and Funaki 1983; Carporzen et al. 2009). More than 90% of the stable NRM carried by chondrules, CAIs and matrix is a middle-temperature (MT) component blocked up to only 290°C even though the meteorite contains grains with blocking temperatures up to ~600°C (Fig. 7A). The paleointensity of the magnetizing field which produced the MT magnetization has been estimated to be 10–100 μT (Butler 1972; Banerjee and Hargraves 1972; Sugiura et al. 1979; Nagata 1979b; Wasilewski 1981; Acton et al. 2007; Carporzen et al. 2009) (the anomalously high paleointensities up to 1600 μT of Lanoix et al. 1978 are highly circumspect given the lack of fusion crust tests and mutual subsample orientation). This component is unidirectional throughout the meteorite despite the lithologic heterogeneity and aggregational texture of the meteorite (Figs. 4a and 7b). Therefore, the MT magnetization was certainly acquired following accretion. Although thermal demagnetization above 300°C indicates that chondrules and refractory inclusions may have a much weaker high-temperature (HT) component oriented nonunidirectionally throughout the meteorite (Sugiura et al. 1979; Sugiura and Strangway 1985; Carporzen et al. 2009) (Fig. 7C), the HT component has not yet been demonstrated to decay to the origin and often does not reach a stable direction. Therefore, the possibility of a preaccretional remanence in Allende, which would be expected to be randomly oriented among individual chondrules, is tantalizing but not yet confirmed.

Although Allende's middle-temperature NRM component has been traditionally interpreted to be a record of solar system magnetic fields generated externally to the CV parent body (Levy and Sonett 1978; Sugiura and Strangway 1988; Nagata 1979b; Acton et al. 2007; Cisowski 1987; Stacey 1976), recent petrographic and geochronological data strongly indicate that it was acquired during slow cooling over several Ma ending at least 8 Ma after the formation of CAIs. This requires that the fields were unidirectional with respect to the parent body over long timescales at a time in solar system history after the likely dissipation of the protoplanetary disk and magnetically active Sun. Therefore, it has recently been concluded that the MT magnetization in Allende is most likely the record of an internal core dynamo active at ~4559–4560 Ma (Carporzen et al. 2009). This would indicate that the meteorite is a partially differentiated object with a chondritic crust and a melted interior including metallic core. Although this represents a radically new picture for chondrite parent bodies, it appears to be consistent with a variety of geochemical data and thermal models for the CV body and may provide a solution to several outstanding but seemingly unrelated problems in meteoritics and planetesimal formation (Elkins-Tanton et al. 2009; Carporzen et al. 2009).

The very limited paleomagnetic analyses available for most other carbonaceous chondrites (including other CVs) have also identified NRM, but this magnetization generally appears to be considerably less stable (lower mean destructive field) compared to Allende. For example, while Allende's whole rock NRM only drops by 10–30% following AF demagnetization to 50 mT (Banerjee and Hargraves 1972; Brecher and Arrhenius 1974; Nagata 1979b; Carporzen et al. 2009), the NRMs of whole rock Orgueil (CI1) and Murchison (CM2) drop by about an order of magnitude after AF demagnetization to 50 mT (Banerjee and Hargraves 1972; Larson et al. 1973; Guskova 1976b, 1978, Kukkonen and Pesonen 1983) (Fig. 8). Directional data (Fig. 10 of Brecher and Arrhenius 1974) suggest that Orgueil has been almost completely demagnetized by this AF level (although their analyzed subsamples may be contaminated with fusion crust magnetization). [Note that Orgueil "sample II" of Banerjee and

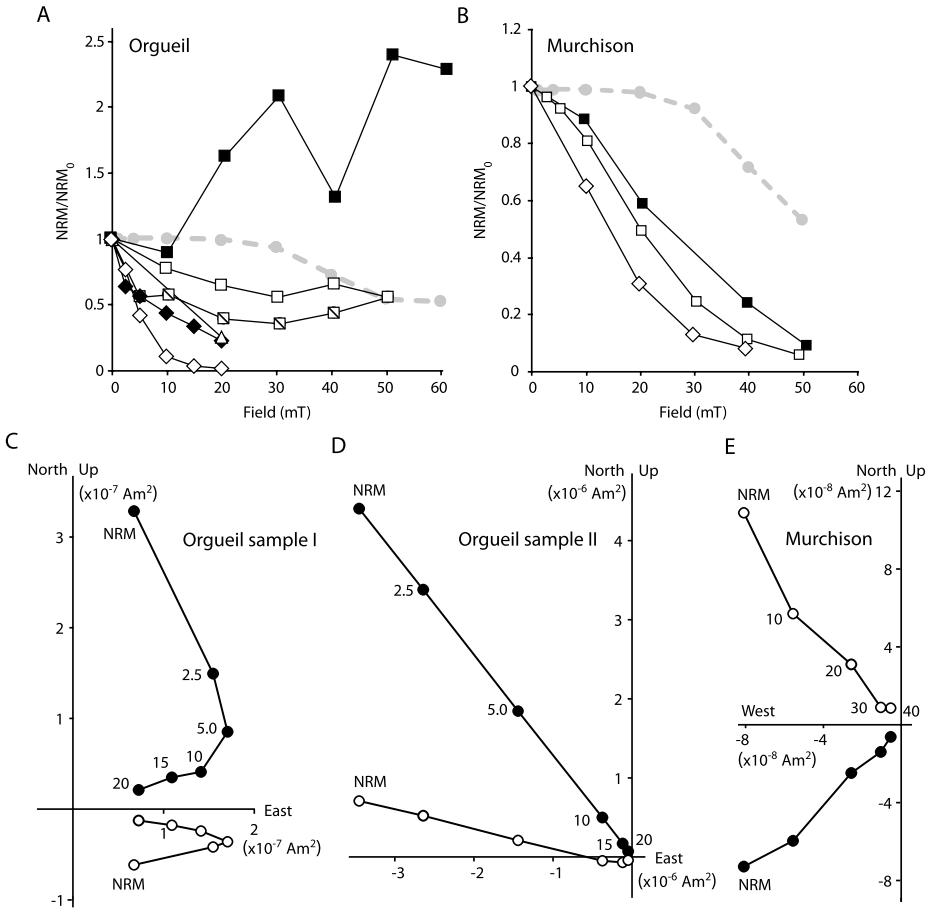

Fig. 8 NRM (normalized to the initial NRM value, NRM_0) in the carbonaceous chondrites Orgueil (CI1) and Murchison (CM2). **A** NRM intensity during AF demagnetization of 6 different bulk subsamples from the interior of Orgueil (no fusion crust). *Squares* = data of Guskova (1976b, 1978). *Diamonds* = data of Banerjee and Hargraves (1971) (*closed symbols* = Orgueil subsample I, *open symbols* = Orgueil subsample II), also shown in **C** and **D**. *Triangles* = data of Nagata (1979e). AF demagnetization data for Allende NRM are shown for context (*grey circles and dashed line*). Data of Guskova (1976b, 1978) (particularly above AF 20 mT) may be contaminated with spurious remanence from AF demagnetization, while Orgueil subsample II appears to be contaminated by secondary IRM (which leads to rapid demagnetization). **B** NRM (normalized to the initial NRM value, NRM_0) intensity during AF demagnetization of 3 different bulk subsamples from the interior of Murchison (no fusion crust). *Squares* = data of Guskova (1976b). *Circles* = data of Banerjee and Hargraves (1971) (*closed symbols* = Murchison subsample 2, *open symbols* = Murchison subsample 1). *Diamonds* = data of Larson et al. (1973), also shown in **E**. AF demagnetization data for Allende NRM are shown for context (*grey circles and dashed line*). **C, D** Orthogonal demagnetization plot of Orgueil subsamples I and II, respectively, computed from data of Banerjee and Hargraves (1971). Open and solid symbols represent projections of the endpoint of the magnetization vectors on vertical and horizontal planes, respectively. Selected demagnetization steps are listed in mT. These two subsamples are apparently not mutually oriented. **E** Orthogonal AF demagnetization plot of Murchison computed from data of Larson et al. (1973). Open and solid symbols represent projections of the endpoint of the magnetization vector on vertical and horizontal planes, respectively. Selected demagnetization steps are listed in mT

Hargraves 1971, which has ∼30 times larger NRM than nearly all other studied Orgueil subsamples—see Fig. 1 of Guskova 1976b and three out of the four Orgueil samples listed in Appendix of Kukkonen and Pesonen 1983—and which demagnetizes straight to the origin (compare Fig. 8D with overprint up to AF 15 mT in Fig. 5B) has likely been remagnetized by a hand magnet or other secondary IRM. Note also that Orgueil subsample 4 and probably also subsample 2 of Guskova 1976b, 1978 may have acquired substantial spurious remanence during AF demagnetization (e.g., Sect. 2.2) as indicated by increasing moment magnitude in Fig. 8A coupled with directional changes toward one of the orthogonal measurement axes in Fig. 4 of Guskova 1976b.]

The NRMs of chondrules from Karoonda (CK4) are demagnetized by 96% by just AF 20 mT. Whole rock Karoonda samples are similarly unstable (Brecher and Arrhenius 1974). Murchison was also found to be much less resistant to thermal demagnetization analyses to 150°C than Allende or Orgueil (Banerjee and Hargraves 1972). Zero-field cycling of these magnetite-rich meteorites to 77 K leads to large changes in NRM intensity (Brecher and Arrhenius 1974; Kletetschka et al. 2003) (with whole rock samples from Karoonda demagnetized by 95%), indicating that Karoonda, Orgueil, and Murchison are highly susceptible to remagnetization and demagnetization effects from thermal cycling in space through magnetite's Verwey transition (see Sect. 2.4). Magnetic viscosity experiments (Kletetschka et al. 2003) suggest nearly all of Murchison's NRM could be accounted for as a VRM acquired in the Earth's field since its arrival on Earth in 1969.

Furthermore, given that Murchison and Orgueil were likely never heated even to ∼150°C (Busemann et al. 2007; Cody et al. 2008) since formation, blocking-temperature relations for magnetite (Pullaiah et al. 1975) and kamacite (Garrick-Bethell and Weiss 2009) indicate that these minerals are unlikely to have retained a primary TRM from the early solar system (4.5 Ga). Only a crystallization remanent magnetization acquired during the formation of magnetite, recently dated to be 4560.3 ± 0.4 Ma (Hohenberg et al. 2000) (essentially contemporaneous with the likely age of Allende's NRM Carporzen et al. 2009), could have persisted from this early time. On the other hand, Karoonda, which has been heavily altered and metamorphosed to estimated temperatures of 500–600°C (Matza and Lipschutz 1977), could in principle retain an ancient TRM, although the age of metamorphism is currently poorly constrained at ∼4500 Ma (Podosek 1970, 1971; Hohenberg et al. 2000). In any case, as described above, the limited data for these meteorites cannot rule out the hypothesis that they formed in near zero-field conditions (see Sect. 7.2). Similarly, Tagish Lake (C2 ungrouped) has a ratio of NRM to saturation IRM (sIRM) of ∼3 to 9×10^{-4} (for 8 samples with masses between 2 to 6000 mg), among the lowest ever measured for any meteorite (Gattacceca's unpublished data), indicating that the high paleointensity published by Gattacceca and Rochette (2004) for this meteorite is attributable to contamination by a hand magnet. Such a scenario would be consistent with the standard paradigm of primitive, undifferentiated parent bodies and a lack of external field sources at the late time when they were thermally and chemically processed. A key way to further test this zero-field hypothesis is to demonstrate that these meteorites can acquire artificial laboratory magnetization (e.g., TRM or ARM) that is much more stable and intense than their NRM (similar to approach of Garrick-Bethell and Weiss 2009 and Lawrence et al. 2008 for lunar rocks).

3.4 Rumuruti-like (R) Chondrites

Rumuruti-like chondrites are a recently recognized highly oxidized, matrix-rich, almost metal-free chondrite group. The paleomagnetism of five bulk Rumuruti chondrites (all Antarctic finds) was studied by Gattacceca and Rochette (2004). All samples had a stable

remanent magnetization mostly carried by pyrrhotite, with the exception of the magnetite-bearing A-881988 meteorite (Rochette et al. 2008). NRM normalization techniques indicated similar paleointensities around ∼5 μT. In view of the pressure-induced magnetic phase transition of pyrrhotite at 2.8 GPa (e.g., Rochette et al. 2003a) and the typical peak shock pressures of Rumuruti chondrites (shock stage S2, with peak pressures >5 GPa), the NRM of Rumuruti chondrites is unlikely to predate the last major impact and must be regarded either as a shock remanent magnetization or, for highly-shocked samples, thermoremanence acquired during post-impact cooling. In either case, the paleointensity estimates suggest the existence of a (possibly transient in the SRM hypothesis) magnetic field at the surface of the Rumuruti parent body at the time of the impact event. Additional detailed paleomagnetic studies of Rumuruti chondrites are needed to infer the origin of this magnetic field.

3.5 Kakangari-like (K) Chondrites

Kakangari-like chondrites are another recently identified chondrite group distinguished by their high matrix and metal contents, oxidation state between H and enstatite chondrites and distinctive oxygen isotopic composition (Weisberg et al. 1996; Krot et al. 2007). We are aware of no paleomagnetic studies of these meteorites.

4 Paleomagnetic Records in Small-Body Stony Achondrites and Mesosiderites

4.1 The Howardite-Eucrite-Diogenite (HED) Clan

The members of the howardite-eucrite-diogenite clan form the most numerous and diverse of the small-body basaltic achondrite groups. Other than lunar and Martian meteorites and an anomalous ureilite (see Sect. 4.4), they are the only achondrites whose parent body (the asteroid 4 Vesta) has been confidently identified. This makes them key samples for studying the early global differentiation, petrogenesis, and the early thermal evolution of planetesimals. However, essentially all known HED meteorites were metamorphosed ≥800°C, brecciated and/or shocked (Metzler et al. 1995; Yamaguchi et al. 1996) at least several tens of Ma (and up to several hundred Ma) after their formation (Bogard and Garrison 2003; Kleine et al. 2005b; Kunz et al. 1995). Therefore, they certainly cannot contain records of early nebular or T Tauri fields. Given that metallic cores are only expected to be convective on Vesta-sized planetesimals for up to <∼100 Ma (Weiss et al. 2008a; Elkins-Tanton et al. 2009), only HEDs with the oldest $^{40}Ar/^{39}Ar$ ages could potentially have retained magnetization from any internal core dynamo. Table 3 lists previous paleomagnetic studies of HEDs and other small-body achondrites.

The dominant ferromagnetic mineral in most HED meteorites is kamacite (Collinson 1994; Collinson and Morden 1994; Rochette et al. 2009a). Analysis of four unbrecciated eucrites found possibly coherent but generally extremely weak NRM, consistent with paleointensities of only order 1–5 μT (Cisowski 1991). The magnetization directions of two mutually oriented subsamples from each of these meteorites appear to be approximately unidirectional (divergent by < ∼30°). Two of these meteorites, PCA 82502 and Moore County, have been dated with $^{40}Ar/^{39}Ar$ chronometry at 4.506 ± 0.033 and 4.48 ± 0.03 Ga, respectively. The former has in fact the oldest known precise $^{40}Ar/^{39}Ar$ age of any eucrite. At face value, this would seem to indicate that there were weak (several μT) magnetic fields on the HED parent body in the vicinity of these meteorites ∼60–80 Ma after the formation of the parent body and solar system. However, because fusion crust baked contact tests

Table 3 Summary of previous paleomagnetic studies of small-body achondrites (excluding irons, pallasites, lunar and Martian meteorites). All names and classifications are as listed in the Meteoritical Bulletin Database with one exception (see below). Other unofficial names are listed in parentheses. Abstracts and unpublished manuscripts were generally excluded unless they were the sole reference for a given meteorite. E = eucrite, D = diogenite, H = howardite, mmict = monomict breccia, pmict = polymict breccia, cm = cumulate unbrecciated, unbr = unbrecciated. Letter and number for mesosiderites give petrologic class and metamorphic grade, respectively (see Hutchison 2004)

Name	Group/Petrologic class	References
Angrites		
A-881371		Weiss et al. (2008a)
Angra dos Reis		Weiss et al. (2008a)
D'Orbigny		Weiss et al. (2008a)
Aubrites		
Bishopville		Brecher et al. (1979), Guskova (1976a, 1984)
Cumberland Falls		Stacey et al. (1961), Larson et al. (1973)
Norton County		Pochtarev and Guskova (1962), Guskova (1976a, 1984), Kukkonen and Pesonen (1983), Gattacceca and Rochette (2004)
Peña Blanca Spring		Gattacceca and Rochette (2004)
Pesyanoe		Pochtarev and Guskova (1962), Guskova (1976a, 1984)
Howardites, eucrites, and diogenites		
DaG 684	E	Gattacceca and Rochette (2004)
ALHA76005	E	Nagata (1979a)
ALHA77302	E-pmict	Nagata (1980), Nagata and Dunn (1981)
ALHA78040	E-pmict	Nagata (1980)
ALHA81001	E-mmict[a]	Cisowski (1991)
FRO 97045	E-pmict	Gattacceca and Rochette (2004)
Juvinas	E-mmict	Pochtarev and Guskova (1962), Guskova (1976a), Brecher et al. (1979), Kukkonen and Pesonen (1983), Gattacceca and Rochette (2004)
Millbillillie	E-mmict	Morden (1992b)
Moore County	E-cm	Lovering (1959), Cisowski (1991)
Nobleboro	E-pmict	Brecher et al. (1979)
Pasamonte[b]	E-pmict	Brecher et al. (1979)
Petersburg	E-pmict[c]	Collinson and Morden (1994)
PCA 82502	E-unbr	Nagata (1979c), Collinson and Morden (1994)
Sioux County	E-mmict	Brecher et al. (1979), Kukkonen and Pesonen (1983), Collinson and Morden 1994
Stannern	E-mmict	Pochtarev and Guskova (1962), Guskova (1976a), Brecher et al. (1979), Kukkonen and Pesonen (1983)
Y-74159	E-mmict	Nagata (1979a, 1979b, 1979c, 1979d, 1979e)
Y-74450	E-pmict	Nagata (1979a, 1979b, 1979c, 1979d, 1979e)
Y-791195	E-cm	Nagata (1979c), Cisowski (1991)
ALHA77256	D	Brecher (1980)
EETA79002	D	Collinson and Morden (1994)
Johnstown	D	Brecher et al. (1979), Kukkonen and Pesonen (1983), Collinson and Morden (1994)

Table 3 (*Continued*)

Name	Group/Petrologic class	References
Roda	D	Brecher et al. (1979), Collinson and Morden (1994)
Shalka	D	Brecher et al. (1979), Collinson and Morden (1994)
Tatahouine	D	Brecher et al. (1979), Gattacceca and Rochette (2004)
Y-74013	D	Sugiura (1977), Nagata (1979a, 1979b, 1979c, 1979e)
Y-74037	D	Nagata (1979d, 1979e)
Y-74097	D	Nagata (1979a, 1979b, 1979e)
Y-74648	D	Nagata (1979a, 1979b, 1979e)
Y-75032	D	Nagata (1979a, 1979b, 1979d, 1979e)
Y-692 (b)	D	Nagata (1979a, 1979b, 1979c, 1979e)
EET 87503	H	Collinson and Morden (1994)
Kapoeta	H	Brecher et al. (1979), Collinson and Morden (1994)
Le Teilleul	H	Brecher et al. (1979), Collinson and Morden (1994)
Luotolax	H	Guskova (1976a)
Pavlovka	H	Pochtarev and Guskova (1962), Guskova (1976a), Brecher et al. (1979)
Yurtuk	H	Pochtarev and Guskova (1962), Guskova (1976a)
Y-7308	H	Nagata (1979c, 1979d)
Mesosiderites		
Bondoc	B4	Larson et al. (1973)
Clover Springs	A2	Larson et al. (1973)
Crab Orchard	A1	Guskova (1965b), Kukkonen and Pesonen (1983)
Estherville	A3/4	Guskova (1965b), Kukkonen and Pesonen (1983), Collinson (1991)
Hainholz	A4	Guskova (1965a, 1965b), Larson et al. (1973)
Mincy	B4	Larson et al. (1973)
Morristown	A3	Guskova (1969), Kukkonen and Pesonen (1983)
Ureilites		
ALHA77257		Nagata (1979e), Brecher (1980), Nagata (1980)
Dyalpur		Brecher (1980), Guskova (1982a)
Goalpara		Larson et al. (1973), Brecher and Fuhrman (1979)
Haverö		Neuvonen et al. (1972), Brecher and Fuhrman (1979), Kukkonen and Pesonen (1983)
Kenna		Brecher and Fuhrman (1979), Guskova (1982a)
Novo-Urei		Pochtarev and Guskova (1962), Larson et al. (1973), Guskova (1976a, 1982a), Kukkonen and Pesonen (1983)
Ungrouped		
GRA 06129		Shearer et al. (2008)
Ibitira[d]		Brecher (1980), Cisowski (1991)

[a]Unbrecciated according to Delaney et al. (1984), Cisowski (1991)

[b]New oxygen isotopic data (Scott et al. 2009) suggest Pasamonte may sample a parent distinct from the other HED meteorites in this table

[c]Classified as a howardite by Collinson and Morden (1994)

[d]Although Ibitira is classified as a eucrite in the Meteoritical Bulletin Database, we follow Mittlefehldt (2007) in classifying it as ungrouped

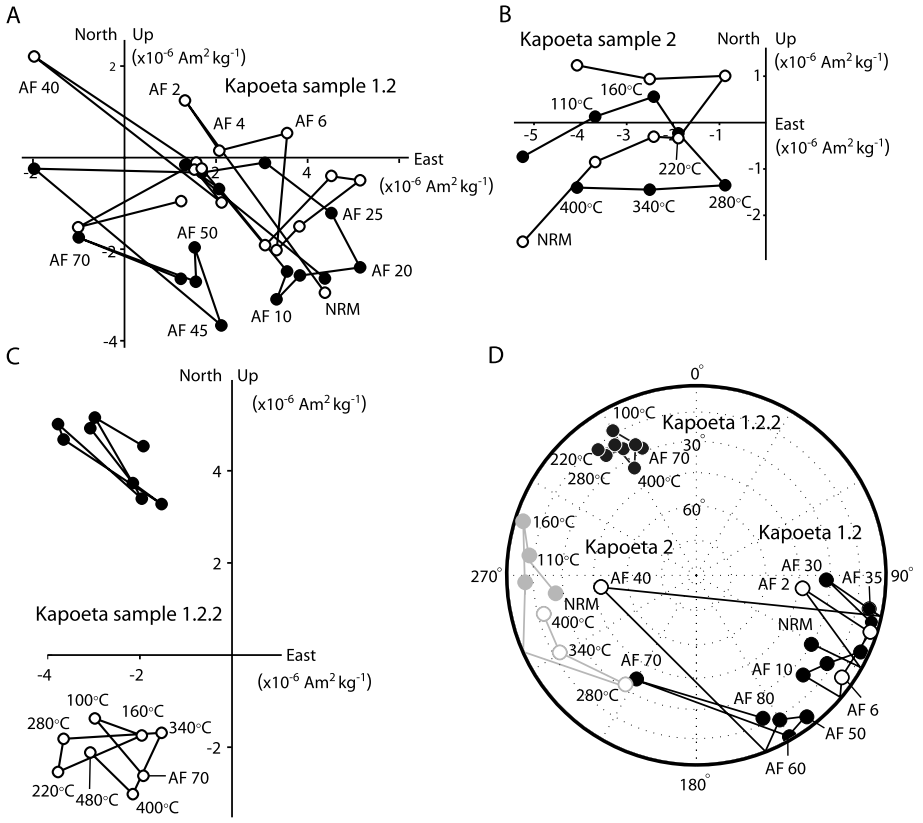

Fig. 9 NRM in three mutually oriented subsamples from the interior of the howardite Kapoeta. **A** Orthogonal projection of the NRM vector of sample 1.2 during AF demagnetization as computed from data of Collinson and Morden (1994). *Open and solid symbols* represent projections of the magnetization vector on vertical and horizontal planes, respectively. Selected demagnetization steps are listed in mT. **B** Orthogonal projection of the NRM vector of sample 2 during thermal demagnetization as computed from data of Collinson and Morden (1994). *Open and solid symbols* represent projections of the magnetization vector on vertical and horizontal planes, respectively. Selected demagnetization steps are listed in °C. **C** Orthogonal projection of the NRM vector of sample 1.2.2 during thermal demagnetization as computed from data of Collinson and Morden (1994). *Open and solid symbols* represent projections of the magnetization vector on vertical and horizontal planes, respectively. Selected demagnetization steps are listed in °C. Sample had been AF demagnetized to 70 mT prior to beginning thermal demagnetization. **D** Equal area stereographic projection of the NRM of each sample shown in **A**–**C** during AF or thermal demagnetization (*black symbols* = sample 1.2, *dark grey symbols* = samples 1.2.2, and *light grey symbols* = sample 2). *Open and solid symbols* represent projections of the magnetization vector on *upper and lower hemispheres*, respectively. Selected demagnetization steps are listed in mT or °C. Samples are mutually oriented

(Sect. 2.6), tests for spurious ARM and GRM remanence acquisition during AF demagnetization (Sect. 2.2), tests for magnetic viscosity, and detailed analysis of shock effects (Sect. 2.3) have not yet been conducted for these samples, this conclusion must be currently regarded as provisional.

The majority of HEDs are breccias and their magnetic carriers have been further strained after brecciation (Gattacceca et al. 2008b). Paleomagnetic analyses of mutually oriented subsamples of most brecciated and unbrecciated HEDs have observed NRMs with widely

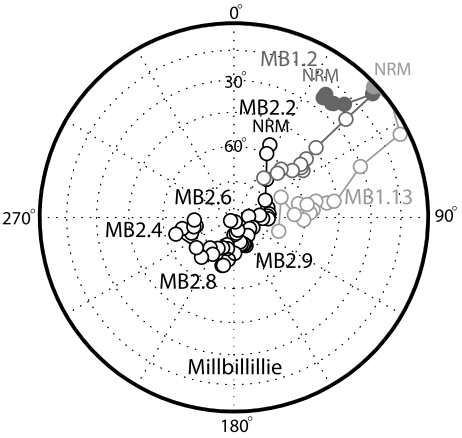

Fig. 10 NRM in seven mutually oriented subsamples from the interior of the eucrite Millbillillie. Shown is an equal area stereographic projection of the magnetization of each sample during AF demagnetization. *Open and solid symbols* represent projections of the magnetization vector on upper and lower hemispheres, respectively. Samples were demagnetized up to 100 mT and reached a stable, nearly vertical final direction. Sample names are listed next to each curve. Samples MB1.13 (*light grey symbols*) and MB1.2 (*dark grey symbols*) have overprints mostly removed by 100 mT, above which their directions are close to that of MB2.2, MB2.4, MB2.6, MB2.8, and MB2.9 (*black symbols*). Adapted from Morden (1992b)

scattered directions and that AF demagnetize erratically (Fig. 9) (Brecher et al. 1979; Collinson and Morden 1994). For the unbrecciated samples, such magnetization is clearly not a primary thermoremanent record. For the brecciated samples, the origin of the NRM is currently ambiguous: the scattered magnetization directions provide a positive conglomerate test demonstrating that the magnetization predates brecciation, indicate poor magnetic recording properties, and/or near-zero fields during the last remagnetization event. The hypothesis of pre-brecciation NRM can be distinguished from the other two mechanisms via identification of origin-trending, unidirectional magnetization within single clasts (e.g., Sugiura and Strangway 1983), a test which the howardite Kapoeta clearly fails (Fig. 9).

In stark comparison, seven mutually oriented subsamples of the Millbillillie eucrite impact melt breccia (Yamaguchi et al. 1994) exhibit a unidirectional magnetization component blocked to at least 100 mT and apparently acquired in a 6–37 μT paleofield (Morden 1992b) (Fig. 10). Given the uncertainty in the paleointensity methodology, this is within error of the paleointensities from unbrecciated eucrites discussed above. However, again, no baked contact tests, tests for spurious ARM and GRM remanence acquisition, and magnetic viscosity tests have been conducted. Assuming future such analyses confirm that the NRM is a primary thermoremanence, then $^{40}Ar/^{39}Ar$ chronometry likely dates this magnetization to the time of impact-induced heating at 3.55 ± 0.02 Ga (Yamaguchi et al. 1994). Although Morden (1992b) interpreted Millbillillie's paleomagnetism as evidence for a core dynamo, this age is so young that it is hard to account for the NRM by anything other than either a remanent crustal field on Vesta or, much less likely, an impact-generated field or close approach to another magnetized body.

4.2 Ibitira

Ibitira is an unbrecciated, vesicular metabasalt that fell in 1957 (Mittlefehldt 2005). Although it was long thought to be an unbrecciated eucrite, oxygen isotopic and major ele-

ment data indicate it may be from a basaltic asteroid other than Vesta (Wiechert et al. 2004; Mittlefehldt 2005). Following metamorphism to peak temperatures of 1100°C, it cooled slowly until it reached the ∼300°C closure temperature for the $^{40}Ar/^{39}Ar$ system at 4.495 ± 0.015 Ga (Bogard and Garrison 1995). Following metamorphism, it was shocked to ∼10–30 GPa (Steele and Smith 1976). These shock effects combined with the 4.495 Ga age of thermoremanence acquisition (which is towards the end of the expected timescale of early dynamo activity; see Sect. 6) may explain why both paleomagnetic studies of mutually oriented subsamples Ibitira found highly nonunidirectional remanence (Cisowski 1991; Brecher 1980). Therefore, Ibitira's paleomagnetic record does not convincingly indicate the presence of a paleomagnetic field.

4.3 Mesosiderites

Mesosiderites are breccias containing clasts of basalt and metal in a fine-grained matrix. They are thought to be the products of the collision of a metal-rich planet onto the basaltic surface of one or more differentiated bodies (Mittlefehldt et al. 1998) or else the impact-induced mixing of the metallic core and silicate mantle on single bodies (Scott et al. 2001). The mineralogy, chemical composition, and oxygen isotopic composition of the silicates suggest that mesosiderites were derived from a parent body similar to (Rubin and Mittlefehldt 1993) or the same as (Greenwood et al. 2006) that of the HED meteorites. Because mesosiderites are shocked, polymict impactites that have experienced multiple episodes of crystallization, melting and metamorphism (Rubin and Mittlefehldt 1993), they make challenging targets for paleomagnetism. Several mesosiderites have been analyzed with AF demagnetization (Larson et al. 1973), but detailed paleomagnetic data have only been reported for Estherville. Analysis of 17 mutually oriented fragments of matrix and metal from Estherville demonstrate found magnetization directions are essentially randomly distributed (Collinson 1991). The major ferromagnetic minerals are kamacite and tetrataenite. Given the complex history of this meteorite, the fact that the matrix samples are themselves composites of smaller clasts, and the unknown method by which tetrataenite acquires NRM, it is not clear how to interpret these data. In any case, the fact that Estherville and other mesosiderites underwent extremely slow cooling (0.1–0.5°C Ma^{-1}) below 500–700°C (Mittlefehldt and Garrison 1998) means that if their NRM is a TRM, it must have been acquired long after any early putative core dynamo or early solar/disk had decayed.

4.4 Ureilites

The ureilites, the second largest group amongst achondrites, are carbon-rich, ultramafic, granular mostly unbrecciated rocks (Mittlefehldt 2007). They contain a variety of ferromagnetic phases, including predominantly kamacite (Rowe et al. 1975; Rochette et al. 2009a) and minor taenite, martensite (in shocked samples), sulfide, suessite (in the shocked North Haig breccia) (Keil et al. 1982), schreibersite, and cohenite (Berkley et al. 1980; Rubin 1997). Recent spectral observations of the meteoroid 2008 TC3 and recovered meteorite samples following its impact on Earth have provisionally tied at least some ureilites to F-type asteroids (Jenniskens et al. 2009). Despite their great number, we are aware of NRM studies of only six ureilites (Larson et al. 1973; Brecher 1980; Brecher and Fuhrman 1979; Nagata 1979e, 1980; Guskova 1982a). We will focus here on Haverö (the only studied fall) and Goalpara, both of which show little evidence of weathering. The dominant ferromagnetic mineral in both meteorites appears to be kamacite (Rowe et al. 1975). Goalpara has been shocked to at least 60 GPa (estimated post-shock temperatures of at least 1100°C)

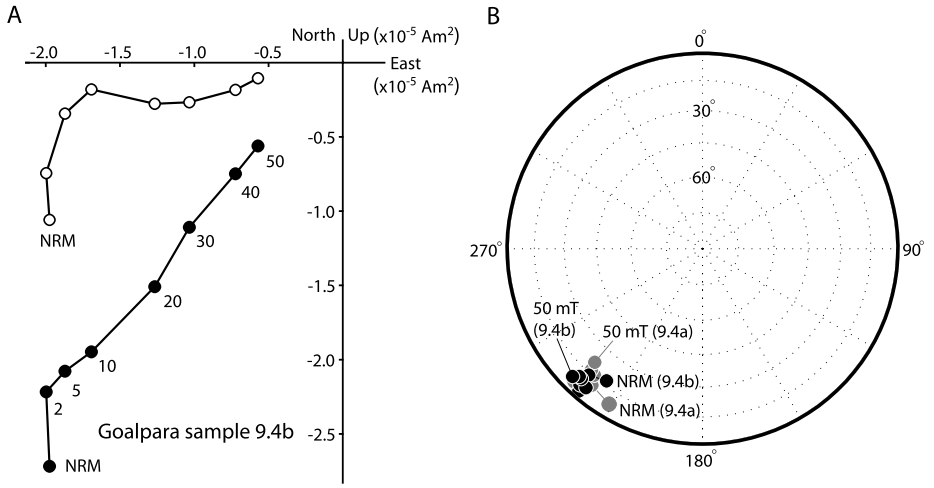

Fig. 11 NRM in two mutually oriented subsamples from the interior of the ureilite Goalpara. **A** Orthogonal projection of the NRM vector of subsample 9.4b during AF demagnetization as computed from data of Brecher and Fuhrman (1979). *Open and solid symbols* represent projections of the magnetization vector on vertical and horizontal planes, respectively. Selected demagnetization steps are listed in mT. **B** Equal area projection showing directions of NRM vector for subsamples 9.4a (*grey circles*) and 9.4b (*black circles*; data also shown in **A**). Selected demagnetization steps are listed in mT. Data from Brecher and Fuhrman (1979)

(Carter et al. 1968; Bischoff and Stoffler 1992) and then apparently thermally annealed. Such an event should have completely thermally remagnetized the rock. Brecher and Fuhrman's analyses of two mutually oriented samples of Goalpara identified a strong NRM with two components: a weak, soft component up to 5 mT and a second dominant component stable up to at least 50 mT that was unidirectional across two mutually oriented subsamples (Brecher and Fuhrman 1979) (Fig. 11). Very similar results were obtained by Larson et al. (1973) for a single chip of Goalpara. Laboratory TRM given to these two subsamples demagnetized at a rate very similar to the high coercivity NRM component. A paleointensity experiment using the AF demagnetization of TRM method (Schwarz 1969; Schwarz and Symons 1970) yielded a paleofield value of 140 μT. Using their measured ratio of NRM to sIRM, we calculate a total REM paleointensity of 34 μT (assuming that the paleofield in microteslas = NRM/sIRM $\times$3000 Gattacceca and Rochette 2004), which is within error of the previous AF of TRM value given the factor of $\sim$3 uncertainties of the REM method (see Kletetschka et al. 2003, 2004a, 2006; Gattacceca and Rochette 2004; Yu 2006; Yu et al. 2007).

Brecher and Fuhrman's (1979) Haverö sample 9.1 has an NRM that is 58% of sIRM and is 20–50 times stronger per unit mass than the two samples studied by Kukkonen and Pesonen (1983); AF demagnetization to 40 mT reduces its intensity by two orders of magnitude. Since no fusion crust baked contact test was conducted, we are suspicious that this subsample may have been remagnetized by a hand magnet. This suspicion also extends to their samples of Kenna, which also have NRMs that are between 13–34% of sIRM and which decay much more rapidly than a laboratory TRM during AF demagnetization. Therefore, at the moment Goalpara is the only ureilite whose paleomagnetism is a good candidate for a thermoremanent record of substantial past magnetic fields. The slow cooling of this meteorite suggests these fields were steady over long timescales and therefore not likely to be of impact origin. The source of this field is at present a mystery given the lack of good

geochronological constraints on ureilites. The primitive nature of ureilites, which show little evidence of siderophile depletion and have highly heterogeneous oxygen isotopic compositions, at present provides little evidence of a possible metallic core on the parent body.

4.5 Aubrites

Aubrites are highly reduced, coarse-grained brecciated achondrites with affinities to enstatite chondrites. The main magnetic carrier in these achondrites is kamacite, although minor amounts of taenite, tetrataenite, schreibersite, and cohenite have been reported (Easton 1986; Rubin 1997; Rochette et al. 2009a). Paleomagnetic studies have only been reported for five aubrites (Stacey et al. 1961; Larson et al. 1973; Brecher et al. 1979; Guskova 1984; Gattacceca and Rochette 2004). Norton County and Pesyanoe possess stable remanent magnetization isolated between 10 and 50 mT. If interpreted as primary TRM acquired during cooling on the aubrite parent body, they indicate a stable paleofield of $\sim$10 μT during cooling below 700°C. However, in view of the brecciated nature of aubrites and their complex shock history (e.g., Sect. 2.3), interpretation of their NRM requires additional studies.

4.6 Angrites

The angrites are a group of twelve basaltic achondrites from an unknown parent body. They are distinguished from other achondrites by three features which make them superb targets for paleomagnetic analysis. Firstly, one of the most important ferromagnetic carriers is magnetite (Weiss et al. 2008a; Rochette et al. 2009a), a mineral whose rock magnetic properties and mode of magnetization acquisition are both simpler and far better understood than those of iron-nickel minerals (for a review, see Dunlop and Ozdemir 1997). Secondly, due to their unusually high U/Pb ratios, they have extremely precise and ancient Pb/Pb ages ranging from ages of 4564–4558 Ma (Amelin 2008; Markowski et al. 2007; Zartman et al. 2006). Thirdly, their state of preservation since final cooling is excellent: they show no evidence for subsequent shock, brecciation, and parent body weathering (Kurat et al. 2004; Prinz et al. 1977; Mittlefehldt et al. 1998; McKay et al. 1988; Kuehner et al. 2006; Yanai 1994) and their (U-Th)/He ages are within error of their Pb/Pb ages for all but two angrites (Busemann et al. 2006). Angrites also have the advantage that their cooling rates (which range from 0.3°C y^{-1} to 10°C h^{-1}) are sufficiently slow to rule out impact-generated or other transient field-generation processes but far faster than that required for tetrataenite formation (in any case, tetrataenite is not favored by the low-nickel content of iron metal in angrites).

Recent paleomagnetic analyses of mutually oriented subsamples of the angrites D'Orbigny (Pb/Pb age 4563.3 $\pm$ 0.1 Ma) and Angra dos Reis (Pb/Pb age 4557.1 $\pm$ 0.1 Ma) (ages from Amelin 2008) identified stable, unidirectional remanent magnetization (Weiss et al. 2008a) (Fig. 12). A fusion crust baked contact test and magnetic viscosity analyses demonstrate that the magnetization in Angra dos Reis is preterrestrial. The lack of shock effects and terrestrial weathering, the high AF stability of the NRM, tests for spurious ARM and GRM acquisition, and low-temperature data indicating the lack of magnetite's Verwey transition collectively indicate that the magnetization is likely a primary TRM dating back to the early solar system. The relatively late age of the meteorite and its slow cooling rate indicate the NRM was acquired too late in solar system history and over too long a time period to have been the product of an external magnetic field from the young sun or protoplanetary nebula. AF paleointensity analyses suggest the field was of order 10–20 μT. Collectively, these data leave magnetization by a core dynamo field as the only compelling hypothesis for producing

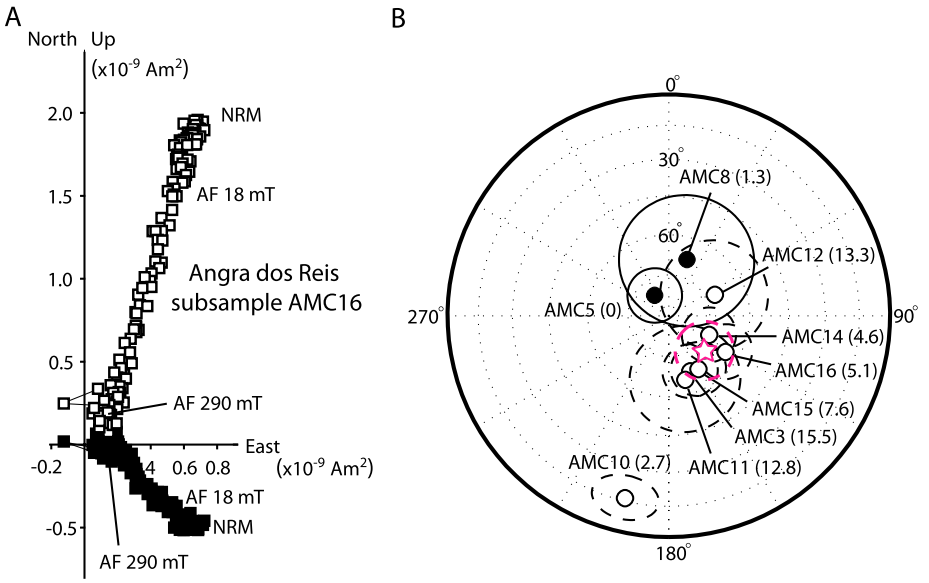

Fig. 12 NRM of the angrite Angra dos Reis. **A** Orthogonal projection showing evolution of NRM vector during AF demagnetization. *Open and closed symbols* represent projections of the endpoint of the magnetization vector on vertical and horizontal planes, respectively. Peak fields for selected AF demagnetization steps are labeled. One main high coercivity component is visible for this subsample. Other interior subsamples have the same HC component sometimes weakly overprinted by a low coercivity secondary component. **B** Fusion crust baked contact test on Angra dos Reis parent sample AMNH. Shown are HC magnetization directions of mutually oriented subsamples ranging from the fusion crusted exterior to the interior (including subsample in **A**), plotted on an equal area stereographic projection. *Closed* (*open*) *symbols* represent projections of vector directions onto *lower* (*upper*) *hemisphere*. Ellipses give estimated orientation uncertainty (either maximum angular deviation of least squares fit or estimated sample positioning uncertainty, whichever is larger). Distance from fusion crust in millimeters is listed next to each sample. Only sample AMC5 contains fusion crust. The seven remaining samples are from the interior, with AMC8 and AMC10 apparently baked by atmospheric passage. Fisher mean direction (*red star*) and associated 95% uncertainty confidence estimate ($\alpha_{95} = 10.7°$) are shown for interior subsamples. The shallow depth of divergent magnetization directions (<3 mm) and the fact that measured samples have NRM/sIRM < 1% throughout their full coercivity range indicate that the exterior has been thermally remagnetized by atmospheric passage rather than isothermally remagnetized by a magnet (see Sects. 2.6 and 2.7). Adapted from Weiss et al. (2008a)

the meteorite's NRM (Weiss et al. 2008a). This is consistent with Hf/W chronometry, which indicates a metallic core formed on the angrite parent body within 3 Ma of solar system formation (Markowski et al. 2007; Kleine et al. 2009).

4.7 Brachinites

Brachinites are olivine-rich cumulates intermediate between differentiated meteorites and primitive achondrites (see below). No paleomagnetic studies have yet been conducted on confirmed brachinites, although recent preliminary paleomagnetic analyses of the ungrouped achondrite GRA 06129, which has oxygen isotopic affinities to brachinites, observed a stable NRM of currently unknown origin (Shearer et al. 2008).

Table 4 Small-body parameters used in the calculations of core heat flux, velocities and magnetic fields. For the electrical conductivity, we use a minimum value from Secco and Schloessin (1989) and we infer the thermal conductivity using the Wiedemann-Franz law. The remaining parameters are from Weiss et al. (2008a). The variables are defined in the text

k	20 W m^{-1} K^{-1}
α	10^{-4} K^{-1}
ρ_c	5000–8000 kg m^{-3}
r_c	10–350 km
$g = 4\pi G r_c \rho_c$	0.04–2.3 m s^{-2}
T	1273 K
C_P	800 J kg^{-1} K^{-1}
σ	6×10^5 S m^{-1}
Ω	2.4×10^{-5}–3×10^{-4} s^{-1}

4.8 Primitive Achondrites

Primitive achondrites are equilibrated, metamorphosed samples that generally have only moderately fractionated chondritic elemental compositions and are not highly differentiated (Mittlefehldt 2007). We are aware of no paleomagnetic analyses of either of the two primitive achondrites clans (acapulcoite-lodranites or winonaite-IAB-iron silicate inclusions) nor of any ungrouped primitive achondrites (e.g., Zag).

5 Dynamo Generation on Small Bodies

The strong primary remanent magnetization present in several angrites (and provisionally identified in other achondrites) may have important implications for the nature of their parent bodies. Most workers consider the angrite parent body to have been an asteroid-sized planetesimal (Mittlefehldt 2007; Mittlefehldt et al. 1998, 2002) although an origin on ancient Mercury has also been discussed (Irving and Kuehner 2007; Ruzicka and Huston 2006). Assuming angrites are remanents of an early solar-system planetesimal, their strong magnetic fields may be the result of cooling in a dynamo-generated field. Here we discuss the feasibility of dynamo generation on small bodies early in solar system history. Using a range of characteristics plausible for these small bodies, we determine whether certain basic criteria for dynamos are met, as well as estimate the resulting core magnetic field strengths.

We consider a body that has differentiated into a core, mantle and crust (Hevey and Sanders 2006) and determine whether its core is susceptible to dynamo action. We will assume that advection is thermally driven (as opposed to compositionally or mechanically driven) such that the core must have a superadiabatic temperature profile in order to generate a dynamo. The heat flux conducted down the core adiabat is given by:

$$F_{\text{cond}} = \frac{k\alpha g T}{C_p} \tag{1}$$

where k is thermal conductivity, α is the thermal expansion coefficient, g is the gravitational acceleration at the core-mantle boundary, C_p is the specific heat and T is the temperature at the core-mantle boundary. The conductive heat flux depends on the core radius r_c and core density ρ_c through the gravitational acceleration g. Using the range of parameter values for small bodies given in Table 4, we find the conductive heat flux lies in the range 1.3×10^{-4} to 7.3×10^{-3} W/m^2.

Thermal evolution modeling has shown that superadiabatic heat fluxes in the range 0.05–0.5 W/m^2 lasting for millions of years were possible for bodies ranging from 70 to 500 km in radius with parameter values similar to those shown in Table 4 (Weiss et al. 2008a). Additionally, cooling rates of parent bodies of iron meteorites have been estimated to be of the order $\mathrm{d}T/\mathrm{d}t = 2$–$6600$ K/Ma from metallographic analyses (Chabot and Haack 2006; Yang and Goldstein 2006; Yang et al. 2008, 2009). The corresponding heat flux at the surface of the metallic core before the onset of crystallization:

$$F = \frac{\rho_c r_c C_P}{3} \frac{\mathrm{d}T}{\mathrm{d}t}$$

is ~0.0008 to 90 W/m^2 for parameters in Table 4, which encompasses the range from thermal evolution models. These are the extreme bounds combining the above range of $\mathrm{d}T/\mathrm{d}t$ estimates with the full range of assumed core radii. For a Vesta-sized body with $r_c = 100$ km and $\mathrm{d}T/\mathrm{d}t = 100$ K/Ma, a representative heat flux value of 0.5 W/m^2 is obtained. It therefore seems likely that small-body cores can maintain thermal convective motions to drive a dynamo early in their histories. It is possible for dynamo action to occur in a body with subadiabatic heat flux if the fluid motions are dominated by mechanical stirring or compositional convection. In a small body, the thermodynamic efficiency of thermal convection is low and compositionally driven convection can be much more efficient in magnetic field generation (Nimmo 2009). However, because these processes are harder to quantify due to uncertainties in the composition of the core and the nature of possible stirring mechanisms, we will ignore these contributions to the fluid motions and only consider a thermally driven dynamo. As such, these calculations strictly apply to dynamos on bodies prior to crystallization of the core. After crystallization has begun, such an approach is conservative if asteroid cores crystallize from the inside outwards, but would overly favor dynamos if cores instead crystallize from the outside inwards (Williams 2009). Because of uncertainties in the phase relations and thermodynamic properties of iron-sulfur alloys neither crystallization regime can be excluded. The way crystallization proceeds in an asteroidal core is a key unresolved problem for understanding dynamos in small bodies.

Producing motions in the core does not guarantee a dynamo. The motions must be three-dimensional and have significantly complex morphologies (for a review of planetary dynamo theory, see Kono and Roberts 2002). We will assume that the convective motions present in these small bodies meet this morphology criterion (as they do in Earth's core). The fluid flows must also be sufficiently rapid to ensure the field is regenerated faster than its ohmic decay. This requires that the magnetic Reynolds number

$$Re_m = \sigma \mu U L$$

exceed a critical value, where σ is electrical conductivity, μ is magnetic permeability, U is a characteristic velocity, and L is a characteristic length scale (e.g., core radius).

Various estimates of lower bounds for the magnetic Reynolds number, Re_m^{crit}, are found in the literature (Roberts and Gubbins 1987). Arguments based on energetics obtain the bound $Re_m^{\mathrm{crit}} e_{\max} > \pi^2$, where $e_{\max}$ is the maximum eigenvalue of the rate of strain tensor. Another bound gives $Re_m^{\mathrm{crit}} > \pi$ where the velocity is based on the maximum velocity in the core. These bounds are lower limits, so the actual critical magnetic Reynolds number may be larger than this. In numerical dynamo models, typically a critical value around 50 is found. However, because these models cannot work in the parameter regime appropriate for planetary and small-body cores, the numerical estimates may not be representative either. In

the following discussion, we consider a critical value of 50 as fairly conservative and allow for the possibility that self-sustained dynamos may operate at $Re_m > 10$.

To estimate the magnetic Reynolds number in our small-body cores, we use the core radius as a characteristic length scale and the electrical conductivity for small-body cores given in Table 4. To determine a characteristic velocity, we use various scaling laws applicable for different force balances in planetary cores. For comparison, the Earth's core ($L \sim 3500$ km) has $Re_m \sim 10^3$ if the secular variation of the field is used to determine the characteristic flow velocities ($U \sim 0.5$ mm/s), suggesting that the Earth has a fairly supercritical magnetic Reynolds number.

We consider three different scaling laws to determine the characteristic velocities for our small bodies. For more information on these and other potential scaling laws, see the paper in this volume by Christensen (2009).

(i) U_{MAC}: This velocity estimate is based on a magnetostrophic balance argument. If the dominant force balance in the core is between the magnetic, Archimedean and Coriolis (MAC) forces, then the velocity scales as

$$U_{\mathrm{MAC}} \sim \left(\frac{2\pi G \alpha r_c F_{\mathrm{conv}}}{C_P \Omega} \right)^{0.5}$$

where Ω is the core angular rotation rate and F_{conv} is the convective heat flux (Stevenson 2003).

(ii) U_{CIA}: This velocity estimate comes from a balance of the non-geostrophic components of the Coriolis, non-linear inertial, and Archimedean (CIA) forces (Aubert et al. 2001; Christensen and Aubert 2006). Geostrophy (Coriolis forces are balanced by pressure gradients) is removed by taking the curl of the momentum equation and therefore eliminating the pressure term resulting in the following velocity estimate:

$$U_{\mathrm{CIA}} \sim \left(\frac{2\sqrt{2}\pi G \alpha}{C_P} \right) \left(\frac{r_c^3 F_{\mathrm{conv}}^2}{\Omega} \right)^{1/5}.$$

(iii) U_{ML}: This velocity estimate is from mixing length theory and assumes a balance between the non-linear inertial and Archimedean forces. It may be appropriate if the convection is highly turbulent and rotation is not a dominant force in the core (Stevenson 2003):

$$U_{\mathrm{ML}} \sim \left(\frac{4\pi G \alpha r_c^2 F_{\mathrm{conv}}}{C_P} \right)^{1/3}$$

where we have assumed that the characteristic length scale is the core radius.

Figure 13 shows regions of parameter space (our varying parameters are the core radius r_c, rotation rate Ω, and convective heat flux F_{conv}) where the magnetic Reynolds number is supercritical for the different velocity scalings. We find a range of supercritical Re_m from all three scalings suggesting that supercritical magnetic Reynolds numbers, and hence dynamos, are quite feasible in small bodies. In general, U_{ML} and U_{CIA} are 1–2 orders of magnitude larger than U_{MAC} and so the magnetic Reynolds numbers based on U_{MAC} are smaller. This is expected since fast rotation (which is assumed in the magnetostrophic balance) inhibits convective motions.

We can also use scaling laws to estimate magnetic field strengths generated by small-body dynamos. There are many scaling laws to choose from in the literature (for a summary

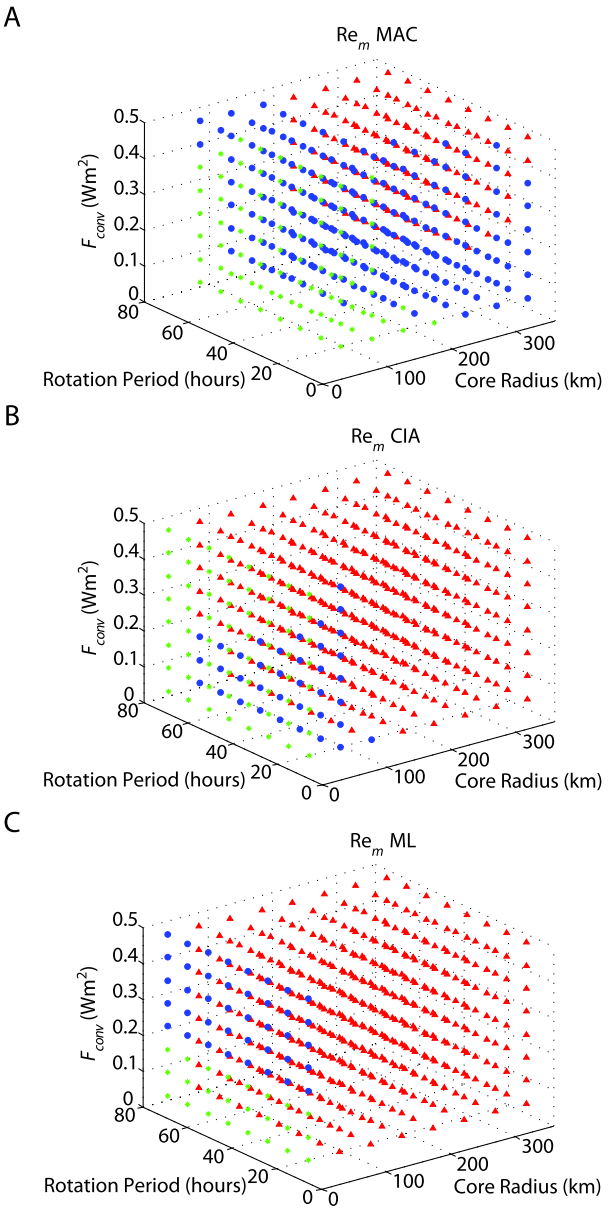

Fig. 13 Parameter values resulting in supercritical Re_m for various velocity scalings. Parameter values resulting in $1 \leq Re_m \leq 10$ are shown in *green stars* (probably no dynamo), $10 < Re_m \leq 50$ are shown in *blue circles* (perhaps a dynamo), and $Re_m > 50$ are shown in *red triangles* (dynamo likely). **A** Uses velocity estimates from the MAC balance, **B** Uses velocity estimates from the CIA balance, and **C** uses mixing length velocity estimates. Core radius is in km, rotation period is in hours, and F_{conv} is in W m^{-2}

see the paper by Christensen in this issue Christensen 2009). We chose two different magnetic field scaling laws related to the force balances from which we derived our velocity estimates. In both of these estimates, we used a core density value of 8000 kg/m^3:

(i) B_{MAC}: This estimate assumes the same force balance as the U_{MAC} estimate (magnetostrophic balance). In this case, if Lorentz and Coriolis forces are comparable, the magnetic field strength is given by:

$$B_{\text{MAC}} \sim (2\Omega\rho_c\mu r_c U_{\text{MAC}})^{0.5}$$

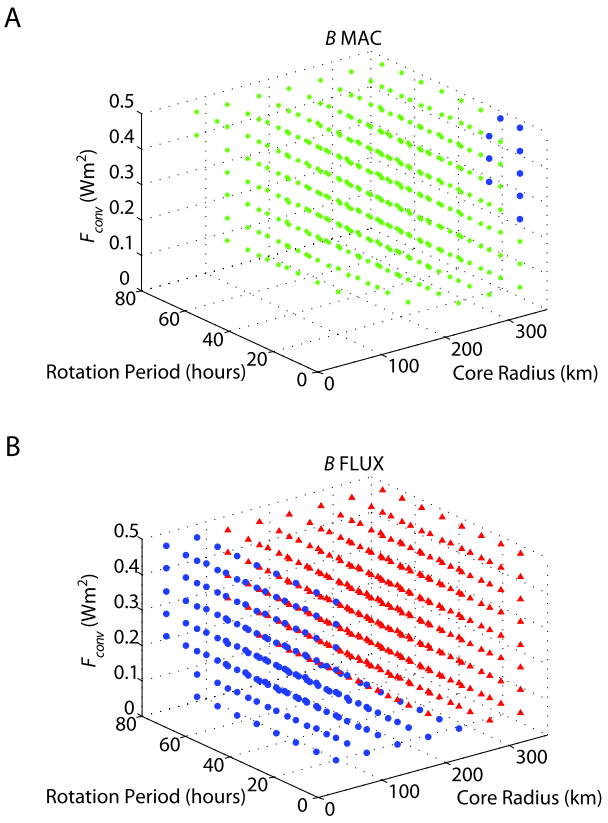

Fig. 14 Core surface magnetic field strengths for parameter values that result in $Re_m > 10$ for the MAC balance (**A**) and the FLUX balance (**B**). Parameter values resulting in $1 \leq B \leq 100$ μT are shown in *green stars*, $100 < B \leq 1000$ μT are shown in *blue circles*, and $B > 1000$ μT are shown in *red triangles*. Core radius is in km, rotation period is in hours, and $F_{\rm conv}$ is in W m^{-2}

(ii) $B_{\rm FLUX}$: This estimate assumes the magnetic field strength is determined by the available power (from the convective heat flux $F_{\rm conv}$) to drive the velocity field:

$$B_{\rm FLUX} \sim \left(\frac{8\pi \mu G \alpha f_{\rm ohm} \rho_c}{C_P} \frac{r_c^2 F_{\rm conv}}{U} \right)^{1/2}$$

where $f_{\rm ohm}$ is the ratio of available power that is lost through ohmic dissipation and is a large fraction of 1 (so we approximate $f_{\rm ohm} = 1$). This magnetic field scaling requires a velocity estimate. Since the mixing length velocities were of the same order of magnitude as the CIA based velocities but with a larger variation, we chose the mixing length velocity in the above scaling (i.e., the range of values found using the $U_{\rm CIA}$ estimates is covered in the range of values found using the $U_{\rm ML}$ values).

Figure 14 demonstrates the range of core magnetic field strengths for the small-body parameters that produced supercritical magnetic Reynolds numbers (where we chose our critical magnetic Reynolds number to be 10). The MAC balance scaling predicts core magnetic fields in the range 0.1–150 μT. The power balance scaling predicts core magnetic field strengths in the range 100–2600 μT.

In the case of the angrites, paleomagnetic studies have determined that the magnetizing field had an intensity of ∼20 μT (Weiss et al. 2008a). In order to compare observations of magnetic field strengths in meteorites to our small-body estimates, the planetary surface

magnetic field strength must be determined from the core magnetic field strength. This requires that we take into account two factors: (i) the ratio of poloidal field strength B_p at the CMB to total field strength $B_{\rm tot}$ in the core, and (ii) the distance from the surface to the core. Assuming $B_p \sim 0.1 B_{\rm tot}$ (based on Earth observations and dynamo models), and a range of core to surface radius ratios (see Weiss et al. 2008a), we find small-body parameters that have both supercritical Re_m and $B_{\rm sur} > 20$ μT, and hence are capable of explaining angrite paleomagnetism. It is therefore quite plausible that angrite paleomagnetism was the product of a dynamo operating in a small parent body early in solar system history.

In addition to the angrites, the estimated range of small-body parameters capable of sustaining dynamo action early in solar system history suggests that many remnants from this time period (such as asteroids and other meteorites) might contain remanent crustal magnetization. With the number of bodies in the asteroid belt, measurements of asteroid crustal magnetic fields could provide a wealth of information to constrain planetary dynamo processes, the critical magnetic Reynolds number, and scaling laws. Our testbed for planetary dynamo processes could increase from the current value of approximately 10 planets and large moons, to hundreds of small bodies.

For example, we consider three of the largest asteroids in the asteroid belt, two of which are soon to be visited by the Dawn mission: Vesta ($r \sim 250$ km), Pallas ($r \sim 270$ km) and Ceres ($r \sim 487$ km). Spectroscopic observations indicate that Vesta has a basaltic surface (McCord et al. 1970) and Hf/W chronometry of HED meteorites indicates it formed a metallic core within 3–4 Ma of solar system formation (Kleine et al. 2004). Although Ceres and Pallas both appear to have chondritic surfaces (McCord and Sotin 2005; Schmidt et al. 2009), a recent geophysical analysis of Ceres could not rule out the possibility that it is a partially differentiated object with small metallic core. It is reasonable that at least Vesta, and possibly Ceres or Pallas, could have core radii in the range of favorable dynamo conditions we considered above and hence that they have remanent crustal fields from dynamo action in their early history. Unfortunately, the Dawn mission is not carrying a magnetometer and therefore will not be able to measure magnetic fields directly. However, the possibility of using surface space weathering characteristics to infer the presence of crustal magnetic fields has been suggested (Vernazza et al. 2006).

Assuming that the conditions for dynamo operation in Vesta or Ceres are satisfied, scaling laws can be used to estimate the topology of the magnetic field. The ratio of inertial to Coriolis forces has been found to have a controlling influence on field geometry: when rotational forces dominate, the field tends to be dipolar, but when inertial forces are relatively important, the magnetic field is dominated by higher multipoles with a fairly white spectrum at the surface of the dynamo (Sreenivasan and Jones 2006; Christensen and Aubert 2006). The ratio of the two forces is expressed by a Rossby number: $Ro = U/(\Omega L)$. Using Vesta's rotation rate of $\Omega = 3 \times 10^{-4}$ s^{-1}, assuming a core heat flux of 300 mW m^{-2}, resulting in a characteristic CIA velocity scaling of 1 mm/s, and assuming a core radius of 100 km (consistent with astronomical observations and meteorite data for Vesta Ruzicka et al. 1997; Ruzicka et al. 2001; Hilton 2002) as a length scale results in $Ro \sim 10^{-5}$, much less than one and suggesting the magnetic field should be dipolar. However, Christensen and Aubert (2006) found that a local Rossby number defined with a characteristic length scale l of the flow, $Ro_l = U/(\Omega l)$, provides better discrimination between dynamo regimes, which is dipolar for $Ro_l < 0.12$ and multipolar for $Ro_l > 0.12$. Olson and Christensen (2006) give a dependence of the local Rossby number on various physical parameters derived from numerical dynamo models, $Ro_l \approx F_{\rm conv}^{1/2} \eta^{1/5} \kappa^{-1/5} \nu^{-1/3} r_c^{-1/3} \Omega^{-7/6}$ where $\eta = (\sigma \mu)^{-1}$ is the magnetic diffusivity, $\kappa = k/(\rho C_P)$ is the thermal diffusivity and ν is the kinematic viscosity. Using parameters from Table 4 along with $\nu = 10^{-6}$ m^{2}s^{-1}, the local Rossby number

is estimated to be approximately 0.5, and hence should operate in the multipolar regime. There is a large degree of uncertainty associated with this statement, because the estimated value does not far exceed the transitional value of 0.12 and some of the parameter values used are highly uncertain. In addition, the scaling law of Olson and Christensen (2006) for Ro_l is purely empirical and depends on viscosity and thermal diffusivity, whose values in the numerical models on which the scaling has been based are far removed from those in planetary cores.

Our illustration using characteristic values for Vesta or Ceres demonstrates that measurements of asteroidal magnetic fields by future missions could provide a wealth of information on asteroid interiors as well as provide useful constraints for planetary dynamo theory.

6 Open Questions

6.1 Origin of Heterogeneous Magnetization

A puzzling aspect of the paleomagnetism of meteorites is the small-scale (down to millimeters in some meteorites) heterogeneity of NRM directions. As discussed above, this heterogeneity has been observed in ordinary chondrites, enstatite chondrites, HED achondrites, as well as in a Martian meteorite (Kirschvink et al. 1997; Collinson 1997; Weiss et al. 2008b) and lunar rocks (Collinson 1985). Several mechanisms could potentially explain this unusual phenomenon: (1) low-temperature accretion of previously magnetized magnetic grains, (2) brecciation by impacts, or (3) tetrataenite formation. However, none of these mechanisms is applicable to all the above-mentioned meteorites. Mechanism 1 does not hold for meteorites that were metamorphosed to temperatures in excess of the Curie temperatures of these grains (for instance, the Bensour meteorite in Gattacceca et al. 2003). Mechanism 2 does not hold for unbrecciated meteorites (e.g., Ibitira in Cisowski 1991 and some of the ordinary chondrites in Morden 1992a). Moreover in some brecciated meteorites, the randomness of NRM is observed at scales smaller than that of the brecciation. Mechanism 3 does not hold for tetrataenite-free meteorites (e.g., HED meteorites in Collinson and Morden 1994). As a consequence, it seems unavoidable that small scale NRM scatter has a different origin in the different meteorites in which it was observed. This scatter not only has important implications for the mode of origin and age of the NRM, but also for the accuracy of paleointensity methods: measurements of bulk samples with primary but nonunidirectional TRM (e.g., due to cold brecciation), would only place lower limits on the true fine-scale NRM and paleointensity (Wasilewski et al. 2002; Weiss et al. 2008b).

6.2 Zero-Field Magnetization

A fourth related explanation for nonunidirectional NRM (Sect. 6.1) is that the magnetization was acquired in an extremely weak magnetic field with interplanetary intensity ($\sim$nT) and therefore is not a robust paleomagnetic record. Being able to determine when a rock has such "zero-field magnetization" is critical since it serves as the null hypothesis for extraterrestrial paleomagnetism. As described above, samples with candidate zero-field primary magnetization include Murchison (CM2), Orgueil (CI1), and Tagish Lake (C2 ungrouped) the Ibitira achondrite, and possibly some HED and ordinary chondrites.

Two key difficulties with identifying zero-field magnetization are that all ferromagnetic grains will have spontaneous moments that cannot be demagnetized and also that the demagnetization process (particularly via AF methods; Sect. 2.2) always introduce some spurious remanence. There have been some previous theoretical attempts to predict expected NRM intensities from zero-field effects (e.g., Irving et al. 1961; Dickson 1962; Kristjansson 1973; Brecher 1976), but these have thus far been unable to quantitatively account for the relatively strong remanence levels in most meteorites. Such calculations need to be more thoroughly pursued in the future.

6.3 Origin of Young Magnetization

Magnetization has been identified in a number of meteorites with relatively young $^{40}Ar/^{39}Ar$ ages (e.g., the Millbillillie eucrite; Sect. 4.1). If this magnetization is confirmed to be a primary record dating back to time of $^{40}Ar/^{39}Ar$ closure, this does not leave many possible explanations for the magnetic field source. One possibility is that of magnetization by remanent crustal magnetic anomalies. This hypothesis could be tested for young eucrites via observations of space weathering effects on Vesta (Vernazza et al. 2006). A second possibility is SRM acquired in an impact-generated or -amplified magnetic field.

7 Conclusions

- Demonstration of preterrestrial TRM in meteorites can be accomplished via a combination of fusion crust baked contact tests, observation of unidirectional magnetization directions from analysis of mutually oriented subsamples, tests for viscous magnetic contamination in the Earth's field and spurious remanence acquisition during demagnetization, demonstration of the lack of shock effects, analysis of thermal stability of NRM carriers over solar system history, and precise geochronometry and thermochronometry.
- Such analyses have been performed in paleomagnetic studies of only a few meteorites. As a result, most meteorites have not yet been definitively shown to contain TRM records of early solar system fields. Two important exceptions are the angrites, a pristine basaltic achondrite group, and Allende, an extremely well-studied CV carbonaceous chondrite. Both meteorites appear to record parent body magnetic fields instead of early external magnetic fields from the T Tauri sun and protoplanetary nebula. The magnetization of several other meteorites including CI and ordinary chondrites is provisionally consistent with a lack of magnetic fields present during their formation.
- Theoretical analyses indicate that many early planetesimals were likely capable of generating short-lived core dynamos. The intensity and timing of these fields are consistent with paleomagnetic observations of angrites and Allende. Therefore paleomagnetism provides paleogeophysical evidence for planetesimal differentiation within just several Ma of solar system formation.

Acknowledgements B.P. Weiss thanks the NASA Mars Fundamental Research Program, the NASA Lunar Advanced Science and Exploration Research Program, the NASA Lunar Science Institute, the NASA Planetary Major Equipment Program, the NSF Instrumentation and Facilities Program, the Charles E. Reed Faculty Initiatives Award fund, the MIT-France Seed Funds program and the Victor P. Starr Professorship fund for support. J. Gattacceca was supported by grant ANR-05-JCJC-0133 and the MIT-France Seed Funds program.

References

G. Acton, Q.Z. Yin, K.L. Verosub, L. Jovane, A. Roth, B. Jacobsen, D.S. Ebel, J. Geophys. Res. **112** (2007). doi:10.1029/2006JB004655

M.H. Acuña, G. Kletetschka, J.E.P. Connerney, in *The Martian Surface: Composition, Mineralogy, and Physical Properties*, ed. by J.F. Bell (Cambridge University Press, Cambridge, 2008), pp. 242–262

A. Al-Kathiri, B.A. Hofmann, A.J.T. Jull, E. Gnos, Meteorit. Planet. Sci. **40**, 1215–1239 (2005)

A.D. Al-Rawas, A.M. Gismelseed, A.A. Yousif, M.E. Elzain, M.A. Worthing, A. Al-Kathiri, E. Gnos, B.A. Hofmann, D.A. Steele, Planet. Space Sci. **55**, 859–863 (2007)

Y. Amelin, Geochim. Cosmochim. Acta **72**, 221–232 (2008)

Y. Amelin, A.N. Krot, Meteorit. Planet. Sci. **42**, 1321–1335 (2007)

E. Anders, N. Grevesse, Geochim. Cosmochim. Acta **53**, 197–214 (1989)

V. Anyzeski, Pop. Astron. **57**, 249–250 (1949)

N. Artemieva, B. Ivanov, Icarus **171**, 84–101 (2004)

J. Aubert, D. Brito, H.-C. Nataf, P. Cardin, J.-P. Masson, Phys. Earth Planet. Inter. **128**, 51–74 (2001)

S.A. Balbus, Annu. Rev. Astron. Astrophys. **41**, 555–597 (2003)

S.A. Balbus, in *Physical Processes in Circumstellar Disks Around Young Stars*, ed. by P. Garcia (University of Chicago Press, Chicago, 2009, in press)

S.K. Banerjee, R.B. Hargraves, Earth Planet. Sci. Lett. **10**, 392–396 (1971)

S.K. Banerjee, R.B. Hargraves, Earth Planet. Sci. Lett. **17**, 110–119 (1972)

J.L. Berkley, G.J. Taylor, K. Keil, G.E. Harlow, M. Prinz, Geochim. Cosmochim. Acta **44**, 1579–1597 (1980)

N.S. Bezaeva, P. Rochette, J. Gattacceca, R.A. Sadykov, V.I. Trukhin, Geophys. Res. Lett. **34**, L23202 (2007). doi:23210.21029/22007GL031501

N.S. Bezaeva, J. Gattacceca, P. Rochette, R.A. Sadukyov, V.I. Trukhin, Phys. Earth Planet. Inter. (2009, in press)

A. Bischoff, D. Stoffler, Eur. J. Mineral. **4**, 707–755 (1992)

P.A. Bland, F.J. Berry, T.B. Smith, S.J. Skinner, C.T. Pillinger, Geochim. Cosmochim. Acta **60**, 2053–2059 (1996)

P.A. Bland, F.J. Berry, C.T. Pillinger, Meteorit. Planet. Sci. **33**, 127–129 (1998)

P.A. Bland, A.W.R. Bevan, A.J.T. Jull, Quat. Res. **53**, 131–142 (2000)

P.A. Bland, M.E. Zolensky, G.K. Benedix, M.A. Sephton, in *Meteorites and the Early Solar System II*, ed. by D.S. Lauretta, H.Y. McSween (The University of Arizona Press, Tucson, 2006), pp. 853–867

D.D. Bogard, D.H. Garrison, Geochim. Cosmochim. Acta **59**, 4317–4322 (1995)

D.D. Bogard, D.H. Garrison, Meteorit. Planet. Sci. **38**, 669–710 (2003)

A.J. Brearley, R.H. Jones, in *Planetary Materials*, ed. by J.J. Papike (Mineralogical Society of America, Washington, 1998), pp. 3-1–3-398

A. Brecher, Earth Planet. Sci. Lett. **29**, 131–145 (1976)

A. Brecher, Lunar Planet. Sci. **11**, 106–108 (1980)

A. Brecher, L. Albright, J. Geomag. Geoelectr. **29**, 379–400 (1977)

A. Brecher, G. Arrhenius, J. Geophys. Res. **79**, 2081–2106 (1974)

A. Brecher, M. Fuhrman, Moon Planets **20**, 251–263 (1979)

A. Brecher, L. Leung, Phys. Earth Planet. Inter. **20**, 361–378 (1979)

A. Brecher, R.P. Ranganayaki, Earth Planet. Sci. Lett. **25**, 57–67 (1975)

A. Brecher, J. Stein, M. Fuhrman, Moon **17**, 205–216 (1977)

A. Brecher, M. Fuhrman, J. Stein, Moon Planets **20**, 265–279 (1979)

V.F. Buchwald, R.S. Clarke, Am. Mineral. **74**, 656–667 (1989)

H. Busemann, S. Lorenzetti, O. Eugster, Geochim. Cosmochim. Acta **70**, 5403–5425 (2006)

H. Busemann, C.M.O.D. Alexander, L.R. Nittler, Meteorit. Planet. Sci. **42**, 1387–1416 (2007)

R.F. Butler, Earth Planet. Sci. Lett. **17**, 120–128 (1972)

R.F. Butler, *Paleomagnetism: Magnetic Domains to Geologic Terranes* (Blackwell Scientific Publications, Boston, 1992), p. 319

L. Carporzen, B.P. Weiss, D.S. Ebel, J. Gattacceca, D.L. Shuster (2009, submitted)

N.L. Carter, C.B. Raleigh, P.S. DeCarli, J. Geophys. Res. **73**, 5439–5461 (1968)

N.L. Chabot, H. Haack, in *Meteorites and the Early Solar System II*, ed. by D.S. Lauretta, H.Y. McSween (University of Arizona, Tucson, 2006), pp. 747–771

U.R. Christensen, Space Sci. Rev. (2009, this issue)

U.R. Christensen, J. Aubert, Geophys. J. Int. **166**, 97–114 (2006)

C.S. Cisowski, in *Geomagnetism*, vol. 2, ed. by J.A. Jacobs (Academic Press, London, 1987), pp. 525–560

C.S. Cisowski, M.D. Fuller, Y.M. Wu, M.F. Rose, P. Wasilewski, Proc. Lunar Planet. Sci. Conf. **6**, 3123–3141 (1975)

S.M. Cisowski, Earth Planet. Sci. Lett. **107**, 173–181 (1991)

S.M. Cisowski, M. Fuller, J. Geophys. Res. **83**, 3441–3458 (1978)
S.M. Cisowski, J.R. Dunn, M. Fuller, Y.M. Wu, M.F. Rose, P.J. Wasilewski, Proc. Lunar Sci. Conf. **7**, 3299–3320 (1976)
R.S. Clarke, E.R.D. Scott, Am. Mineral. **65**, 624–630 (1980)
G.D. Cody, C.M.O.D. Alexander, H. Yabuta, A.L.D. Kilcoyne, T. Araki, H. Ade, P. Dera, M. Fogel, B. Militzer, B.O. Mysen, Earth Planet. Sci. Lett. **272**, 446–455 (2008)
D.W. Collinson, *Methods in Rock Magnetism and Paleomagnetism* (Chapman and Hall, New York, 1983), p. 503
D.W. Collinson, Earth Moon Planet. **33**, 31–58 (1985)
D.W. Collinson, Earth Planet. Sci. Lett. **84**, 369–380 (1987)
D.W. Collinson, Meteoritics **26**, 1–10 (1991)
D.W. Collinson, Adv. Space Res. **8**, 227–237 (1992)
D.W. Collinson, Philos. Trans. R. Soc. Lond. A **349**, 197–207 (1994)
D.W. Collinson, Meteorit. Planet. Sci. **32**, 803–811 (1997)
D.W. Collinson, S.J. Morden, Earth Planet. Sci. Lett. **126**, 421–434 (1994)
D.A. Crawford, P.H. Schultz, Nature **336**, 50–52 (1988)
D.A. Crawford, P.H. Schultz, J. Geophys. Res. **96**, 18807–18817 (1991)
D.A. Crawford, P.H. Schultz, Int. J. Impact. Eng. **14**, 205–216 (1993)
D.A. Crawford, P.H. Schultz, Int. J. Impact. Eng. **23**, 169–180 (1999)
P.H.M. Dankers, J.D.A. Zijderveld, Earth Planet. Sci. Lett. **53**, 89–92 (1981)
I. de Pater, J.J. Lissauer, *Planetary Sciences* (Cambridge University Press, Cambridge, 2001), p. 528
J.S. Delaney, M. Prinz, C.E. Nehru, C.P. Stokes, Lunar Planet. Sci. **15**, 212–213 (1984)
S.J. Desch, H.C. Connolly, Meteorit. Planet. Sci. **37**(2), 183–207 (2002)
S.J. Desch, J.N. Cuzzi, Icarus **143**, 87–105 (2000)
T.L. Dickinson, P. Wasilewski, Meteorit. Planet. Sci. **35**(1), 65–74 (2000)
G.O. Dickson, J. Geophys. Res. **67**, 4943–4945 (1962)
R.R. Doell, C.S. Gromme, A.N. Thorpe, F.E. Senftle, Science **167**, 695–697 (1970)
D.J. Dunlop, J. Geophys. Res. **111**, B12S02 (2006). doi:10.1029/2006JB004572
D.J. Dunlop, O. Ozdemir, *Rock Magnetism: Fundamentals and Frontiers* (Cambridge University Press, New York, 1997), p. 573
A.J. Easton, Meteoritics **21**, 79–93 (1986)
L.T. Elkins-Tanton, B.P. Weiss, M.T. Zuber (2009, submitted)
S.S. Fonton, Meteoritika **11**, 121–122 (1954)
J. Fritz, N. Artemieva, A. Greshake, Meteorit. Planet. Sci. **40**, 1393–1411 (2005)
M. Fuller, Rev. Geophys. Space Phys. **12**, 23–69 (1974)
M. Fuller, S.M. Cisowski, in *Geomagnetism*, vol. 2, ed. by J.A. Jacobs (Academic Press, Orlando, 1987), pp. 307–455
M.D. Fuller, in *Encyclopedia of Geomagnetism and Paleomagnetism*, ed. by D. Gubbins, E. Herrero-Bervera (Springer, Dordrecht, 2007), pp. 788–801
M. Funaki, J. Magn. Soc. Jpn. **29**, 918–925 (2005)
M. Funaki, N. Nakamura, Antartic Meteorites **XXVII**, 21–22 (2002)
M. Funaki, Y. Syono, Meteorit. Planet. Sci. **43**, 1–13 (2008)
M. Funaki, T. Nagata, K. Momose, Mem. Natl. Inst. Polar Res. **20**(Spec. Issue), 300–315 (1981)
I. Garrick-Bethell, B.P. Weiss, Earth Planet. Sci. Lett. (2009, submitted)
I. Garrick-Bethell, B.P. Weiss, D.L. Shuster, J. Buz, Science **323**, 356–359 (2009)
J. Gattacceca, P. Rochette, Earth Planet. Sci. Lett. **227**, 377–393 (2004)
J. Gattacceca, P. Rochette, M. Bourot-Denise, Phys. Earth Planet. Inter. **140**, 343–358 (2003)
J. Gattacceca, P. Rochette, M. Denise, G. Consolmagno, L. Folco, Earth Planet. Sci. Lett. **234**, 351–368 (2005)
J. Gattacceca, M. Boustie, B.P. Weiss, P. Rochette, E.A. Lima, L.E. Fong, F.J. Baudenbacher, Geology **34**, 333–336 (2006)
J. Gattacceca, A. Lamali, P. Rochette, M. Boustie, L. Berthe, Phys. Earth Planet. Inter. **162**, 85–98 (2007)
J. Gattacceca, L. Berthe, M. Boustie, F. Vadeboin, P. Rochette, T. De Resseguier, Phys. Earth Planet. Inter. **166**, 1–10 (2008a)
J. Gattacceca, P. Rochette, M. Gounelle, M. van Ginneken, Earth Planet. Sci. Lett. **270**, 280–289 (2008b)
S.A. Gilder, M. Le Goff, Geophys. Res. Lett. **35**, L10302 (2008). doi:10310.11029/12008GL033325
S.A. Gilder, M. Le Goff, J.-C. Chervin, High Pressure Res. **26**, 539–547 (2006)
J.L. Gooding, in *International Workshop on Antarctic Meteorites*. LPI Technical Report, vol. 86-01 (Lunar and Planetary Science Institute, Houston, 1986), pp. 48–54
R.C. Greenwood, I.A. Franchi, A. Jambon, J.A. Barrat, T.H. Burbine, Science **313**, 1763–1765 (2006)
Y.G. Guskova, Geomagn. Aeron. **3**, 308–312 (1963)

Y.G. Guskova, Meteoritika **26**, 60–65 (1965a)
Y.G. Guskova, Geomagn. Aeron. **5**, 91–96 (1965b)
Y.G. Guskova, Meteoritika **29**, 116–127 (1969)
Y.G. Guskova, Meteoritika **30**, 74–87 (1970)
Y.G. Guskova, *The Magnetic Properties of Meteorites*. NASA Technical Translation TT F-792 (National Aeronautics and Space Administration, Washington, 1976a)
Y.G. Guskova, Meteoritika **35**, 78–86 (1976b)
Y.G. Guskova, Meteoritika **37**, 144–151 (1978)
Y.G. Guskova, Meteoritika **40**, 61–66 (1982a)
Y.G. Guskova, Meteoritika **41**, 44–49 (1982b)
Y.G. Guskova, Meteoritika **42**, 119–137 (1983)
Y.G. Guskova, Meteoritika **43**, 155–160 (1984)
Y.G. Guskova, Meteoritika **44**, 111–118 (1985)
Y.G. Guskova, Meteoritika **46**, 94–96 (1987)
Y.G. Guskova, Meteoritika **47**, 137–142 (1988)
Y.G. Guskova, V.I. Pochtarev, in *Meteorite Research*, ed. by P.M. Millman (Reidel, Dordrecht, 1969), pp. 633–637
H. Haack, T.J. McCoy, in *Treatise on Geochemistry*, vol. 1, ed. by H.D. Holland, K.K. Turekian (Elsevier, Amsterdam, 2007), pp. 1–22
J.M. Herndon, The Magnetization of Carbonaceous Chondrites, in Geochemistry, PhD Texas, A&M University (1974), p. 114
J.M. Herndon, M.W. Rowe, E.E. Larson, D.E. Watson, Earth Planet. Sci. Lett. **29**, 283–290 (1976)
P.J. Hevey, I.S. Sanders, Meteorit. Planet. Sci. **41**, 95–106 (2006)
R. Hide, Moon **4**, 39 (1972)
J.L. Hilton, in *Asteroids III*, ed. by W.F. Bottke, A. Cellino, P. Paolicchi, R.P. Binzel (University of Arizona Press, Tucson, 2002), pp. 103–112
C.M. Hohenberg, O.V. Pravdivtseva, A. Meshik, Geochim. Cosmochim. Acta **64**, 4257–4262 (2000)
L.L. Hood, Geophys. Res. Lett. **14**, 844–847 (1987)
L.L. Hood, N.A. Artemieva, Icarus **193**, 485–502 (2008)
L.L. Hood, C.S. Cisowski, Rev. Geophys. Space Phys. **21**, 676–684 (1983)
S. Hu, E. Appel, V. Hoffmann, W.W. Schmahl, S. Wang, Geophys. J. Int. **134**, 831–842 (1998)
R. Hutchison, *Meteorites: A Petrologic, Chemical, and Isotopic Synthesis* (Cambridge University Press, Cambridge, 2004), p. 506
A.J. Irving, S.M. Kuehner, in *Workshop on Chronology of Meteorites and the Early Solar System*, abstract #4050 (2007)
E. Irving, P.M. Stott, M.A. Ward, Philos. Mag. **6**, 225–241 (1961)
P. Jenniskens, M.H. Shaddad, D. Numan, S. Elsir, A.M. Kudoda, M.E. Zolensky, L. Le, G.A. Robinson, J.M. Friedrich, D. Rumble, A. Steele, S.R. Chesley, Nature **458**, 485–488 (2009)
A. Johansen, in *Cosmic Magnetic Fields: From Planets, to Stars and Galaxies*, ed. by K.G. Strassmeier, A.G. Kosovichev, J.E. Beckman. Proc. IAU Symp., vol. 259 (2009), pp. 119–128
M.K.R. Joung, M.-M. Mac Low, D.S. Ebel, Astrophys. J. **606**, 532–541 (2004)
G.W. Kallemeyn, A.E. Rubin, J.T. Wasson, Geochim. Cosmochim. Acta **60**, 2243–2256 (1996)
K. Keil, J.L. Berkley, L.H. Fuchs, Am. Mineral. **67**, 126–131 (1982)
J.L. Kirschvink, A.T. Maine, H. Vali, Science **275**, 1629–1633 (1997)
J.L. Kirschvink, R.E. Kopp, T.D. Raub, Geochem. Geophys. Geosyst. **9**, Q05Y01 (2008). doi:10.1029/2007GC001856
T. Kleine, K. Mezger, C. Münker, H. Palme, A. Bischoff, Geochim. Cosmochim. Acta **68**, 2935–2946 (2004)
T. Kleine, K. Mezger, H. Palme, E. Scherer, C. Munker, Geochim. Cosmochim. Acta **69**, 5805–5818 (2005)
T. Kleine, B. Bourdon, A.J. Irving, Lunar Planet. Sci. **40**, abstract #2403 (2009)
G. Kletetschka, T. Kohout, P.J. Wasilewski, Meteorit. Planet. Sci. **38**, 399–405 (2003)
G. Kletetschka, M.H. Acuna, T. Kohout, P.J. Wasilewski, J.E.P. Connerney, Earth Planet. Sci. Lett. **226**, 521–528 (2004a)
G. Kletetschka, J.E.P. Connerney, N.F. Ness, M.H. Acuna, Meteorit. Planet. Sci. **39**, 1839–1848 (2004b)
G. Kletetschka, M.D. Fuller, T. Kohout, P.J. Wasilewski, E. Herrero-Bervera, N.F. Ness, M.H. Acuna, Phys. Earth Planet. Inter. **154**, 290–298 (2006)
T. Kohout, F. Donadini, L.J. Pesonen, M. Uehara, Geophysica **46**, 3–19 (2010)
T. Kohout, G. Kletetschka, M. Kobr, P. Pruner, P.J. Wasilewski, Phys. Chem. Earth **29**, 885–897 (2004)
T. Kohout, G. Kletetschka, L.J. Pesonen, P.J. Wasilewski, Lunar Planet. Sci. **37**, abstract #1601 (2006)
M. Kono, P.H. Roberts, Rev. Geophys. **40**, 1013 (2002). doi:1010.1029/2000RG000102
L. Kristjansson, Tellus **25**, 300–304 (1973)

A.N. Krot, M.I. Petaev, E.R.D. Scott, B.-G. Choi, M.E. Zolensky, K. Keil, Meteorit. Planet. Sci. **33**, 1065–1085 (1998)
A.N. Krot, K. Keil, E.R.D. Scott, C.A. Goodrich, M.K. Weisberg, in *Treatise on Geochemistry*, vol. 1, ed. by H.D. Holland, K.K. Turekian (Elsevier, Amsterdam, 2007), pp. 1–52
S.M. Kuehner, A.J. Irving, T.E. Bunch, J.H. Wittke, G.M. Hupe, A.C. Hupe, Lunar Planet. Sci. **37**, abstract #1344 (2006)
I.T. Kukkonen, L.J. Pesonen, Bull. Geol. Soc. Finland **55**, 157–177 (1983)
J. Kunz, M. Trieloff, K.D. Bobe, D. Stöffler, E.K. Jessberger, Planet. Space Sci. **43**, 527–543 (1995)
G. Kurat, M.E. Varela, F. Brandstatter, G. Weckwerth, R.N. Clayton, H.W. Weber, L. Schultz, E. Wasch, M.A. Nazarov, Geochim. Cosmochim. Acta **68**, 1901–1921 (2004)
M. Lanoix, D.W. Strangway, G.W. Pearce, Proc. Lunar Sci. Conf. **8**, 689–701 (1977)
M. Lanoix, D.W. Strangway, G.W. Pearce, Geophys. Res. Lett. **5**, 73–76 (1978)
E.E. Larson, D.E. Watson, J.M.R. Herndon, J. Geomag. Geoelectr. **25**, 331–338 (1973)
K. Lawrence, C. Johnson, L. Tauxe, J. Gee, Phys. Earth Planet. Inter. (2008). doi:10.1016/j.pepi.2008.1005.1007
M.R. Lee, P.A. Bland, Geochim. Cosmochim. Acta **68**, 893–916 (2004)
M.R. Lee, C.L. Smith, S.H. Gordon, M.E. Hodson, Meteorit. Planet. Sci. **41**, 1123–1268 (2006)
F.Y. Levinson-Lessing, in *Selected Works*, vol. 3 (USSR Academy of Sciences Press, 1952), pp. 363–366
E.H. Levy, S. Araki, Icarus **81**, 74–91 (1989)
E.H. Levy, C.P. Sonett, in *Protostars and Planets: Studies of Star Formation and of the Origin of the Solar System*, ed. by T. Gehrels (University of Arizona Press, Tucson, 1978), pp. 516–532
K.L. Louzada, S.T. Stewart, B.P. Weiss, Geophys. Res. Lett. **34**, L05204 (2007). doi:05210.01029/02006GL027685
K.L. Louzada, S.T. Stewart, B.P. Weiss, J. Gattacceca, N.S. Bezaeva, Earth Planet. Sci. Lett. (2009, submitted)
J.F. Lovering, Am. J. Sci. **257**, 271–275 (1959)
J.F. Lovering, in *Researches on Meteorites*, ed. by C.B. Moore (Wiley, New York, 1962), pp. 179–197
A. Markowski, G. Quitte, T. Kleine, A.N. Halliday, M. Bizzarro, A.J. Irving, Earth Planet. Sci. Lett. **262**, 214–229 (2007)
S.D. Matza, M.E. Lipschutz, Geochim. Cosmochim. Acta **41**, 1398–1401 (1977)
T.B. McCord, J.B. Adams, T.V. Johnson, Science **168**, 1445–1447 (1970)
T.B. McCord, C. Sotin, J. Geophys. Res. **110**, E05009 (2005). doi:05010.01029/02004JE002244
G. McKay, D. Lindstrom, S.-R. Yang, J. Wagstaff, Lunar Planet. Sci. **19**, 762–763 (1988)
K. Metzler, K.D. Bobet, H. Palme, B. Spettel, D. Stöffler, Planet. Space Sci. **43**, 499–525 (1995)
D.W. Mittlefehldt, Meteorit. Planet. Sci. **40**, 665–677 (2005)
D.W. Mittlefehldt, in *Treatise on Geochemistry*, vol. 1, ed. by H.D. Holland, K.K. Turekian (Elsevier, Amsterdam, 2007), pp. 1–40
D.W. Mittlefehldt, D.H. Garrison, Geochim. Cosmochim. Acta **62**, 1459–1468 (1998)
D.W. Mittlefehldt, T.J. McCoy, C.A. Goodrich, A. Kracher, in *Planetary Materials*, ed. by J.J. Papike (Mineralogical Society of America, Chantilly, 1998), pp. 4-1–4-195
D.W. Mittlefehldt, M. Killgore, M.T. Lee, Meteorit. Planet. Sci. **37**, 345–369 (2002)
M. Miyamoto, H. Takeda, K. Yanai, Mem. Natl. Inst. Polar Res. **8**(Spec. Issue), 170–184 (1978)
S.J. Morden, Phys. Earth Planet. Inter. **71**, 189–204 (1992a)
S.J. Morden, Meteoritics **27**, 560–567 (1992b)
S.J. Morden, D.W. Collinson, Earth Planet. Sci. Lett. **109**, 185–204 (1992)
T. Nagata, Proc. Lunar Planet. Sci. Conf. **10**, 2199–2210 (1979a)
T. Nagata, Phys. Earth Planet. Inter. **20**, 324–341 (1979b)
T. Nagata, Mem. Natl. Inst. Polar Res. **12**(Spec. Issue), 238–249 (1979c)
T. Nagata, Mem. Natl. Inst. Polar Res. **15**(Spec. Issue), 253–272 (1979d)
T. Nagata, Mem. Natl. Inst. Polar Res. **15**(Spec. Issue), 280–293 (1979e)
T. Nagata, Mem. Natl. Inst. Polar Res. **17**(Spec. Issue), 233–242 (1980)
T. Nagata, Phys. Earth Planet. Inter. **26**, 125–133 (1981)
T. Nagata, Proc. Lunar Planet. Sci. Conf. **13**, A779–A784 (1983)
T. Nagata, in *Primitive Solar Nebula and Origin of Planets*, ed. by H. Oya (Terra Scientific Publishing Company, Tokyo, 1993), pp. 89–103
T. Nagata, B.J. Carleton, Proc. Jpn. Acad. B **65**, 121–124 (1989)
T. Nagata, J.R. Dunn, Mem. Natl. Inst. Polar Res. **20**(Spec. Issue), 333–344 (1981)
T. Nagata, M. Funaki, Mem. Natl. Inst. Polar Res. **25**(Spec. Issue), 222–250 (1982)
T. Nagata, M. Funaki, Mem. Natl. Inst. Polar Res. **30**(Spec. Issue), 403–434 (1983)
T. Nagata, M. Funaki, Mem. Natl. Inst. Polar Res. **46**(Spec. Issue), 245–262 (1987)
T. Nagata, M. Funaki, Antartic Meteorites **XIV**, 160–163 (1989)

T. Nagata, M. Funaki, J.A. Danon, Mem. Natl. Inst. Polar Res. **41**(Spec. Issue), 364–381 (1986)
T. Nagata, N. Sugiura, Phys. Earth Planet. Inter. **13**(4), 373–379 (1977)
T. Nagata, N. Sugiura, F.C. Schwerer, Mem. Natl. Inst. Polar Res. **5**(Spec. Issue), 91–110 (1975)
T. Nagata, J.A. Danon, M. Funaki, Mem. Natl. Inst. Polar Res. **46**(Spec. Issue), 263–282 (1987)
T. Nagata, M. Funaki, H. Kojima, Proc. NIPR Symp. Antarct. Meteorites **4**, 390–403 (1991)
D. Nesvorný, D. Vokrouhlický, W.F. Bottke, B. Gladman, T. Häggström, Icarus **188**, 400–413 (2007)
K.J. Neuvonen, B. Ohlson, H. Papunen, T.A. Häkli, P. Ramdohr, Meteoritics **7**, 515–531 (1972)
F. Nimmo, Geophys. Res. Lett. **36**, L10201 (2009). doi:10.1029/2009GL037997
I. Nishioka, M. Funaki, T. Sekine, Earth Planets Space **59**, e45–e48 (2007)
P. Olson, U.R. Christensen, Earth Planet. Sci. Lett. **250**, 561–571 (2006)
L.J. Pesonen, M. Terho, I.T. Kukkonen, Proc. NIPR Symp. Antarct. Meteor. **6**, 401–416 (1993)
V.I. Pochtarev, Y.G. Guskova, Geomagn. Aeron. **2**, 626–634 (1962)
F.A. Podosek, Geochim. Cosmochim. Acta **84**, 341–365 (1970)
F.A. Podosek, Geochim. Cosmochim. Acta **35**, 157–178 (1971)
J. Pohl, A. Eckstaller, Lunar Planet. Sci. **12**, 851–853 (1981)
J. Pohl, U. Bleil, U. Hornemann, J. Geophys. **41**, 23–41 (1975)
M. Prinz, K. Keil, P.F. Hlava, J.L. Berkley, C.B. Gomes, W.S. Curvello, Earth Planet. Sci. Lett. **35**, 317–330 (1977)
M.E. Pritchard, D.J. Stevenson, in *Origin of the Earth and Moon*, ed. by R.M. Canup, K. Righter (The University of Arizona Press, Tucson, 2000), pp. 179–196
G. Pullaiah, G. Irving, K.L. Buchan, D.J. Dunlop, Earth Planet. Sci. Lett. **28**, 133–143 (1975)
P.H. Roberts, D. Gubbins, in *Geomagnetism*, vol. 2, ed. by J.A. Jacobs (Academic Press, London, 1987), pp. 185–249
P. Rochette, J.P. Lorand, G. Fillion, V. Sautter, Earth Planet. Sci. Lett. **190**(1–2), 1–12 (2001)
P. Rochette, G. Fillion, R. Ballou, F. Brunet, B. Ouladdiaf, L. Hood, Geophys. Res. Lett. **30**, 1683 (2003a)
P. Rochette, L. Sagnotti, M. Bourot-Denise, G. Consolmagno, L. Folco, J. Gattacceca, M.L. Osete, L. Pesonen, Meteorit. Planet. Sci. **38**, 251–268 (2003b)
P. Rochette, J. Gattacceca, V. Chevrier, V. Hoffmann, J.P. Lorand, M. Funaki, R. Hochleitner, Meteorit. Planet. Sci. **40**, 529–540 (2005)
P. Rochette, J. Gattacceca, V. Chevrier, P.E. Mathé, M. Menvielle, M.S. Team, Astrobiology **6**, 423–436 (2006)
P. Rochette, J. Gattacceca, L. Bonal, M. Bourot-Denise, V. Chevrier, J.-P. Clerc, G. Consolmagno, L. Folco, M. Gounelle, T. Kohout, L. Pesonen, E. Quirico, L. Sagnotti, A. Skripnik, Meteorit. Planet. Sci. **43**, 959–980 (2008)
P. Rochette, J. Gattacceca, M. Bourot-Denise, G. Consolmagno, L. Folco, T. Kohout, L. Pesonen, L. Sagnotti, Meteorit. Planet. Sci. **44**, 405–427 (2009a)
P. Rochette, B.P. Weiss, J. Gattacceca, Elements **5**, 223–228 (2009b)
M.W. Rowe, J.M. Herndon, E.E. Larson, D.E. Watson, NASA Report, NASA-CR-141143 (1975)
A.E. Rubin, Meteorit. Planet. Sci. **32**, 231–247 (1997)
A.M. Rubin, D.W. Mittlefehldt, Icarus **101**, 201–212 (1993)
S.S. Russell, L. Hartmann, J. Cuzzi, A.N. Krot, M. Gounelle, S. Weidenschilling, in *Meteorites and the Early Solar System II*, ed. by D.S. Lauretta, H.Y. McSween (University of Arizona, Tucson, 2006), pp. 233–251
A. Ruzicka, M. Huston, in *69th Annual Meteoritical Society Meeting*, abstract #5080 (2006)
A. Ruzicka, G. Snyder, L.A. Taylor, Meteorit. Planet. Sci. **32**, 825–840 (1997)
A. Ruzicka, G. Snyder, L.A. Taylor, Geochim. Cosmochim. Acta **65**, 979–997 (2001)
S. Sahijpal, P. Soni, G. Gupta, Meteorit. Planet. Sci. **42**, 1529–1548 (2007)
T. Sano, S.-I. Inutsuka, N.J. Turner, J.M. Stone, Astrophys. J. **605**, 321–339 (2004)
B.E. Schmidt, P.C. Thomas, J.M. Bauer, J.-Y. Li, L.A. McFadden, M.J. Mutchler, S.C. Radcliffe, A.S. Rivkin, C.T. Russell, J.W. Parker, S.A. Stern, Science **326**, 275–278 (2009)
H. Schulze, D. Stöffler, Meteoritics **32**, A116 (1997)
E.J. Schwarz, J. Geomag. Geoelectr. **21**, 669–667 (1969)
E.J. Schwarz, D.T.A. Symons, J. Geophys. Res. **75**, 6631–6640 (1970)
E.R.D. Scott, K. Keil, D. Stoffler, Geochim. Cosmochim. Acta **56**, 4281–4293 (1992)
E.R.D. Scott, H. Haack, S.G. Love, Meteorit. Planet. Sci. **36**, 869–881 (2001)
E.R.D. Scott, R.C. Greenwood, I. Franchi, I.S. Sanders, Geochim. Cosmochim. Acta **73**, 5835–5853 (2009)
R.A. Secco, H.H. Schloessin, J. Geophys. Res. **94**, 5887–5894 (1989)
C.K. Shearer, P.V. Burger, C.R. Neal, Z. Sharp, L.E. Borg, L. Spivak-Birndorf, M. Wadhwa, J.J. Papike, J.M. Karner, A.M. Gaffney, J. Shafer, B.P. Weiss, J.W. Geissman, V.A. Fernandes, Am. Mineral. **93**, 1937–1940 (2008)

F.H. Shu, H. Shang, T. Lee, Science **271**(5255), 1545–1552 (1996)
F.H. Shu, H. Shang, A.E. Glassgold, T. Lee, Science **277**(5331), 1475–1479 (1997)
B. Sreenivasan, C.A. Jones, Geophys. J. Int. **164**, 467–476 (2006)
L.J. Srnka, Proc. Lunar Sci. Conf. **8**, 785–792 (1977)
F.D. Stacey, Annu. Rev. Earth Planet. Sci. **4**, 147–157 (1976)
F.D. Stacey, J.F. Lovering, Nature **183**, 529–530 (1959)
F.D. Stacey, J.F. Lovering, L.G. Parry, J. Geophys. Res. **66**, 1523–1534 (1961)
I.M. Steele, J.V. Smith, Earth Planet. Sci. Lett. **33**, 67–78 (1976)
A. Stephenson, J. Geophys. Res. **98**, 373–381 (1993)
D.J. Stevenson, Earth Planet. Sci. Lett. **208**, 1–11 (2003)
N. Sugiura, J. Geomag. Geoelectr. **29**, 519–539 (1977)
N. Sugiura, D.W. Strangway, Proc. Lunar Planet. Sci. Conf. **12**, 1243–1256 (1981)
N. Sugiura, D.W. Strangway, Mem. Natl. Inst. Polar Res. **25**(Spec. Issue), 260–280 (1982)
N. Sugiura, D.W. Strangway, Earth Planet. Sci. Lett. **62**, 169–179 (1983)
N. Sugiura, D.W. Strangway, Proc. Lunar Planet. Sci. Conf. **15**, C729–C738 (1985)
N. Sugiura, D.W. Strangway, in *Meteorites and the Early Solar System*, ed. by J.F. Kerridge, M.S. Mathews (University of Arizona Press, Tucson, 1988), pp. 595–615
N. Sugiura, M. Lanoix, D.W. Strangway, Phys. Earth Planet. Inter. **20**, 342–349 (1979)
N. Sugiura, T. Matsui, D.W. Strangway, Proc. Lunar Planet. Sci. Conf. **16**, 831–832 (1985)
P.C. Thomas, R.P. Binzel, M.J. Gaffey, A.D. Storrs, E.N. Wells, B.H. Zellner, Science **277**, 1492–1495 (1992)
H.C. Urey, Proc. Natl. Acad. Sci. USA **41**, 127–144 (1955)
J.-P. Vallée, New Astron. Rev. **47**, 85–168 (2003)
P. Vernazza, R. Brunetto, G. Strazzulla, M. Fulchignoni, P. Rochette, N. Meyer-Vernet, I. Zouganelis, Astron. Astrophys. **451**, L43–L46 (2006)
P.J. Wasilewski, Moon **6**, 264–291 (1973)
P. Wasilewski, Moon **9**, 335–354 (1974a)
P. Wasilewski, Moon **11**, 313–316 (1974b)
P. Wasilewski, Phys. Earth Planet. Inter. **11**, P5–P11 (1976)
P. Wasilewski, Phys. Earth Planet. Inter. **26**(1–2), 134–148 (1981)
P. Wasilewski, Phys. Earth Planet. Inter. **52**, 150–158 (1988)
P. Wasilewski, Lunar Planet. Sci. **31**, abstract #1454 (2000)
P. Wasilewski, T. Dickinson, Meteorit. Planet. Sci. **35**, 537–544 (2000)
P.J. Wasilewski, C. Saralker, Proc. Lunar Planet. Sci. Conf. **12**, 1217–1227 (1981)
P. Wasilewski, M.H. Acuna, G. Kletetschka, Meteorit. Planet. Sci. **37**, 937–950 (2002)
B. Weaving, Geochim. Cosmochim. Acta **26**, 451–455 (1962a)
B. Weaving, Geophys. J. R. Astron. Soc. **7**, 203–211 (1962b)
M.K. Weisberg, M. Prinz, R.N. Clayton, T. Mayeda, M.M. Grady, I. Franchi, C.T. Pillinger, G.W. Kallemeyn, Geochim. Cosmochim. Acta **60**, 4253–4263 (1996)
M.K. Weisberg, T.J. McCoy, A.N. Krot, in *Meteorites and the Early Solar System II*, ed. by D.S. Lauretta, H.Y. McSween (University of Arizona, Tucson, 2006), pp. 19–52
B.P. Weiss, J.L. Kirschvink, F.J. Baudenbacher, H. Vali, N.T. Peters, F.A. MacDonald, J.P. Wikswo, Science **290**, 791–795 (2000)
B.P. Weiss, H. Vali, F.J. Baudenbacher, J.L. Kirschvink, S.T. Stewart, D.L. Shuster, Earth Planet. Sci. Lett. **201**, 449–463 (2002)
B.P. Weiss, S. Berdahl, L.T. Elkins-Tanton, S. Stanley, E.A. Lima, L. Carporzen, Science **322**, 713–716 (2008a)
B.P. Weiss, L.E. Fong, H. Vali, E.A. Lima, F. Baudenbacher, Geophys. Res. Lett. **35**(23), L23207 (2008b)
M. Westphal, Phys. Earth Planet. Inter. **43**, 300–306 (1986)
M. Westphal, H. Whitechurch, Phys. Earth Planet. Inter. **31**, 1–9 (1983)
G.W. Wetherill, Annu. Rev. Earth Planet. Sci. **18**, 205–256 (1990)
U.H. Wiechert, A.N. Halliday, H. Palme, D. Rumble, Earth Planet. Sci. Lett. **221**, 373–382 (2004)
M.A. Wieczorek, B.L. Jolliff, A. Khan, M.E. Pritchard, B.P. Weiss, J.G. Williams, L.L. Hood, K. Righter, C.R. Neal, C.K. Shearer, I.S. McCallum, S. Tompkins, B.R. Hawke, C. Peterson, J.J. Gillis, B. Bussey, Rev. Mineral. Geochem. **60**, 221–364 (2006)
Q. Williams, Earth Planet. Sci. Lett. **284**, 564–569 (2009)
E.A. Wilson, ISIJ Int. **34**, 615–630 (1994)
A. Yamaguchi, H. Takeda, D.D. Bogard, D.H. Garrison, Meteoritics **29**, 237–245 (1994)
A. Yamaguchi, G.J. Taylor, K. Keil, Icarus **124**, 97–112 (1996)
K. Yanai, Proc. NIPR Symp. Antarct. Geosci. **7**, 30–41 (1994)
J. Yang, J.I. Goldstein, Geochim. Cosmochim. Acta **70**, 3197–3215 (2006)

J. Yang, J.I. Goldstein, E.R.D. Scott, Geochim. Cosmochim. Acta **72**, 3043–3061 (2008)
J. Yang, J.I. Goldstein, J.R. Michael, P.G. Kotula, Lunar Planet. Sci. **40**, abstract #1186 (2009)
Y. Yu, Earth Planet. Sci. Lett. **250**, 27–37 (2006)
Y. Yu, L. Tauxe, J.S. Gee, Earth Planet. Sci. Lett. **162**, 244–248 (2007)
Y. Yu, S.-J. Doh, W. Kim, K. Min, Phys. Earth Planet. Inter. **177**, 12–18 (2009)
R.E. Zartman, E. Jagoutz, S.A. Bowring, Lunar Planet. Sci. **38**, abstract #1580 (2006)